

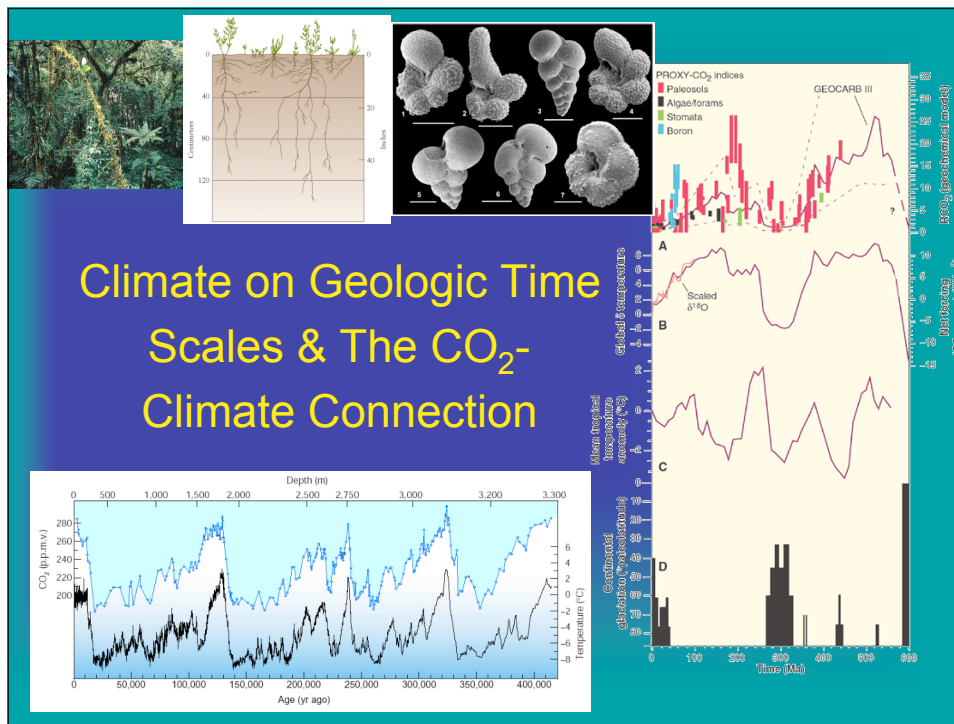
Earth's Climate: the Last 550 Myr

OCEAN 355
Prof. Julian Sachs
Lecture Notes #7
Autumn 2008

Where We've Been & Where We Will Go

- Reviewed what processes control CO₂ greenhouse effect over geologic time (i.e., geochem C cycle)
- And what negative feedbacks (e.g., T-weathering, CO₂-weathering) might keep climate system from reaching &/or remaining in extreme states
- Applied these concepts to understand the Neoproterozoic glaciations (SBEs)
- But the inferences we've made for a strong control of climate by CO₂ (e.g., during Faint Young Sun, SBE) have not been backed by actual data on CO₂ levels *
- Now turn to geologic evidence for CO₂-climate link during last 500 Myr

* Prior to ~550 Ma the lack of animals with hard skeletons & vascular plants results in little or no fossil evidence of atmospheric CO₂ levels.

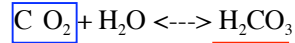


Climate on Geologic Time Scales & The CO₂-Climate Connection

Climate Controls - Long & Short Timescales

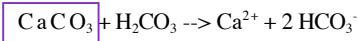
- Solar output (luminosity): 10⁹ yr
- Continental drift (tectonics): 10⁸ yr
- Orogeny (tectonics): 10⁷ yr
- Orbital geometry (Earth -Sun distance): 10⁴-10⁵ yr
- Ocean circulation (geography, climate): 10¹ -10³ yr
- Composition of the atmosphere (biology, tectonics, volcanoes): 10⁰-10⁵ yr

Chemical Weathering = chemical attack of rocks by dilute acid



The **Geochemical** (or non-biological part of the) **Carbon Cycle**

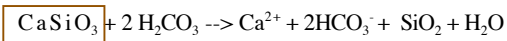
1. Carbonate Weathering:



Carbonate Rocks (e.g., limestone)



2. Silicate Weathering:

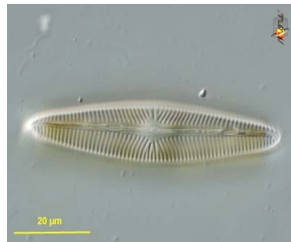


Silicate Rocks (most of the mantle & crust. E.g., granite)

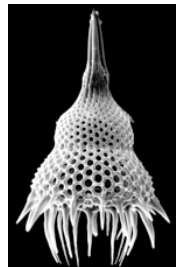


- 2x CO₂ consumption for silicates
- Carbonates weather faster than silicates

http://en.wikipedia.org/wiki/Image:Yosemite_20_bg_090404.jpg http://en.wikipedia.org/wiki/Image:Burren_karst.jpg



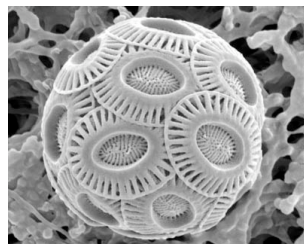
Diatom
(SiO₂)



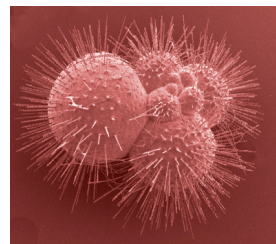
Radiolarian
(SiO₂)

Products of weathering precipitated as CaCO₃ & SiO₂ in ocean

R, Protozoans
L, Eukaryotic Phytoplankton

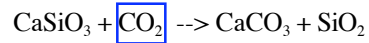


Coccolithophorid
(CaCO₃)



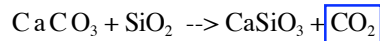
Foraminifer
(CaCO₃)

Net Reaction of Rock Weathering
+
Carbonate and Silica Precipitation in Ocean



- CO₂ consumed (~ 0.03 Gt C/yr)
- Would deplete atmospheric CO₂ in 20 kyr
- Plate tectonics returns CO₂ via Volcanism and Metamorphism

Carbonate Metamorphism

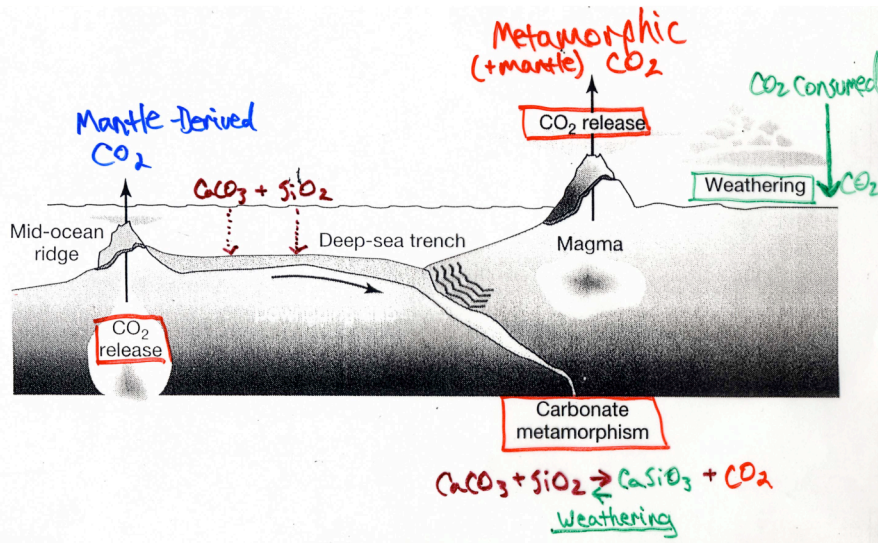


- CO₂ produced from subducted marine sediments

**Net reaction of
geochemical
carbon cycle
(Urey Reaction)**

- On geologic time scales, rock weathering balanced by carbonate metamorphism
- Any *imbalance* can cause changes in atmospheric CO₂

Carbonate-Silicate Geochemical Cycle



Kump et al. (1999)

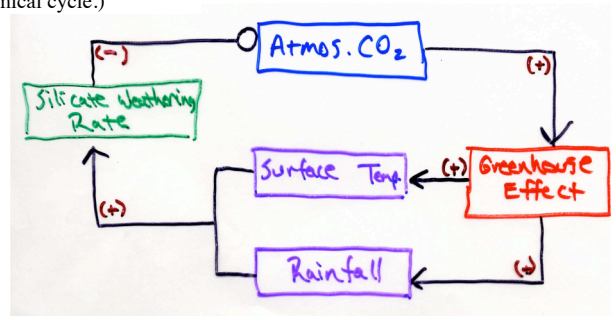
- Geologic record indicates climate has rarely reached or maintained extreme Greenhouse or Icehouse conditions....
- Negative feedbacks between climate and Geochemical Carbon Cycle must exist
- Thus far, only identified for Carbonate-Silicate Geochemical Cycle:

Temp., rainfall enhance weathering rates
(Walker et al, 1981)

(I.e., no obvious climate dependence of tectonics or organic carbon geochemical cycle.)

How are CO₂ levels kept in balance?

Feedbacks



Adapted from Kump et al. (1999)

→Facts:

- Trace atmospheric gas that efficiently traps outgoing IR

→Hypotheses and theories:

- Solution to FYSP
- Through influence on CO₂: weathering, tectonics and organic carbon burial/oxidation control climate on geologic timescales
- Negative feedbacks:
 1. Temp. – Weathering
 2. CO₂ - Weathering

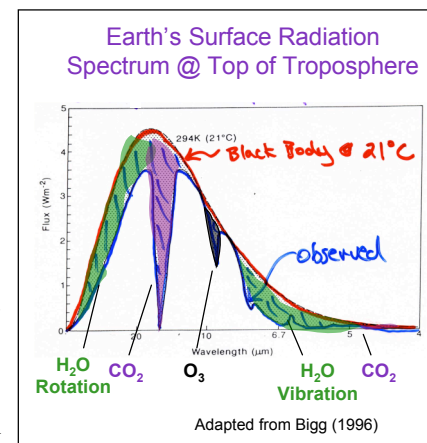
→Tests:

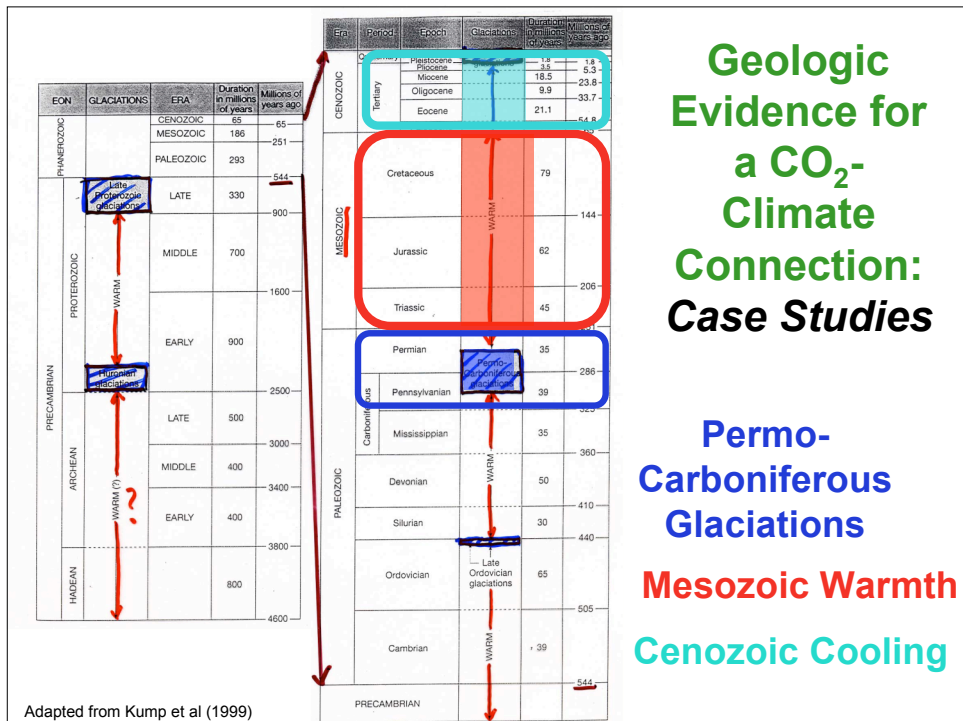
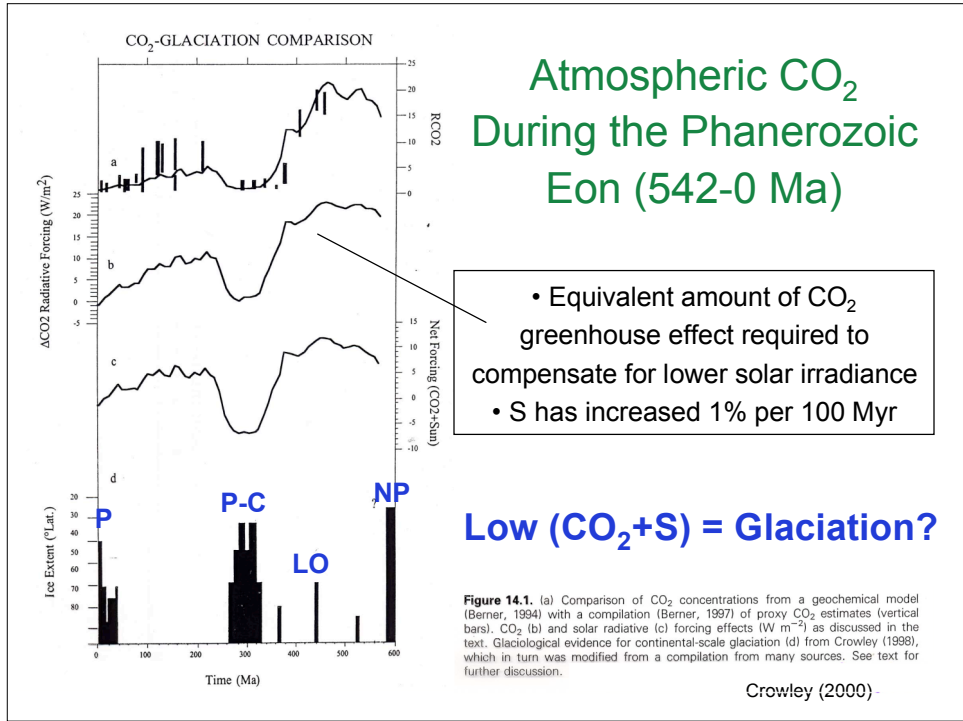
- Comparisons between "proxies" for CO₂ and T

→State of the science:

- Substantial support for close link... with notable exceptions....

The CO₂-Climate Connection





Permo-Carboniferous Glaciations (~300-275 Ma)



Stanley (2000)

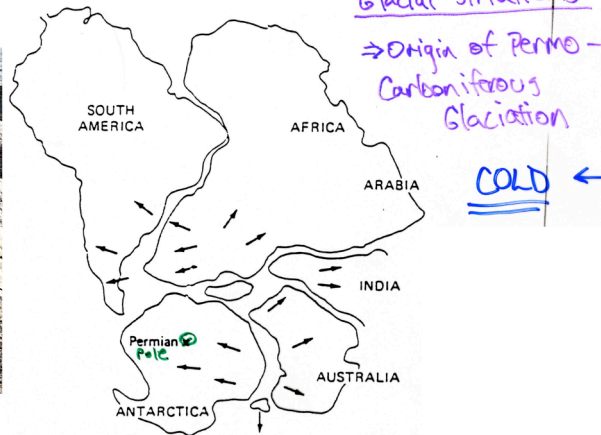
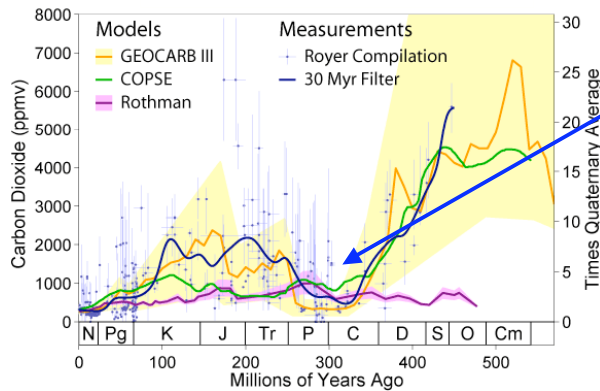


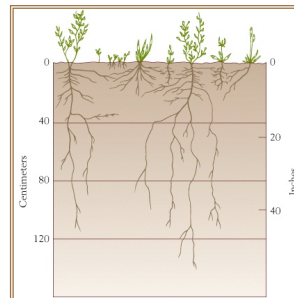
Fig. 11.11. Generalized diagram illustrating evidence for origination of Permo-Carboniferous glaciation on one large landmass. Arrows indicate direction of glacial flow. X = Permian pole position. [After Sullivan, 1974] Reproduced by permission from W. Sullivan, "Continents in Motion: The New Earth Debate," copyright 1974, McGraw-Hill Publishing Co.

Phanerozoic CO₂ Evolution



• Permo-Carboniferous Glaciations Followed a period of marked CO₂ decline

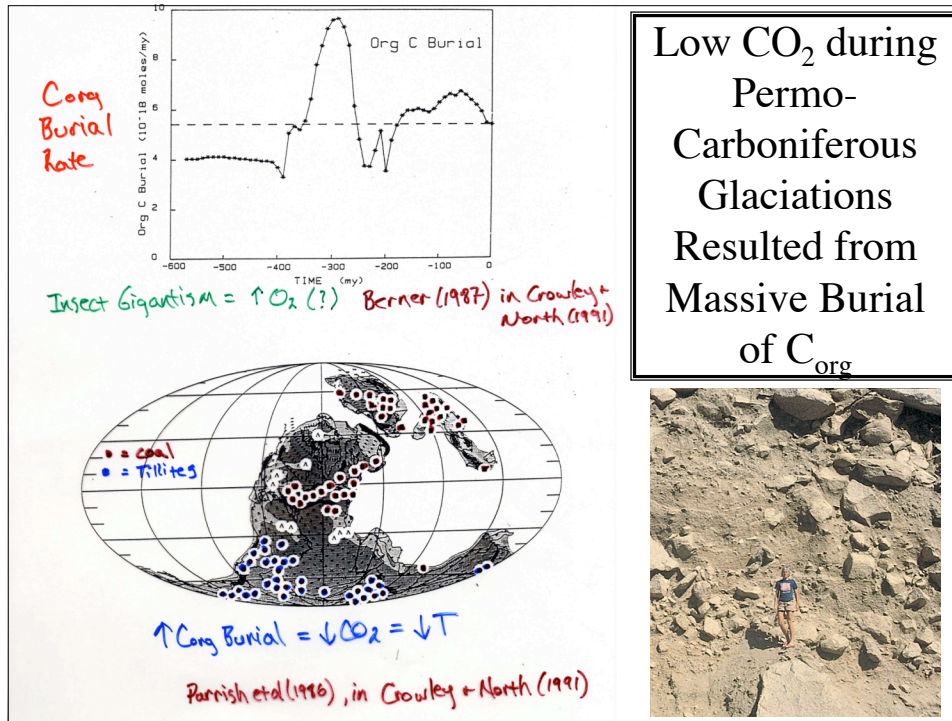
- CO₂ decline likely resulted from spread of rooted vascular plants in the Devonian, 400-360 Ma.
- Dissolution of bedrock (weathering) from: secreted acids, metabolic CO₂ from C_{org} decomposition, & anchoring of clay-rich soil to rock (which retains water).



Stanley (2000)

Theory: Berner (1997) *Science*, Vol. 276: 544-547
http://www.globalwarmingart.com/wiki/Image:Phanerozoic_Carbon_Dioxide_png

*** Ended Here 11/19/08 ***



Insect Gigantism: *Meganeura monyi*

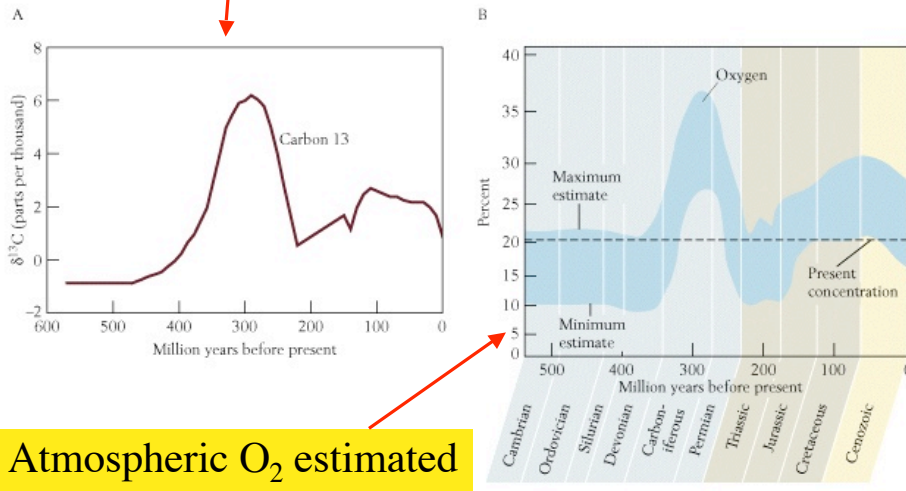
← →
> 0.75 m

Meganeura in BBC's Walking With Monsters

- *Meganeura monyi* was a prehistoric insect of the Carboniferous period (300 million years ago), resembling and related to the present-day dragonfly. With a wingspan of more than 75 cm (2.5 ft) wide, it was the largest known flying insect species to ever appear on Earth. (The Permian *Meganeuropsis permiana* is another contender). It was predatory, feeding on other insects and even small amphibians.

<http://en.wikipedia.org/wiki/Meganeura>

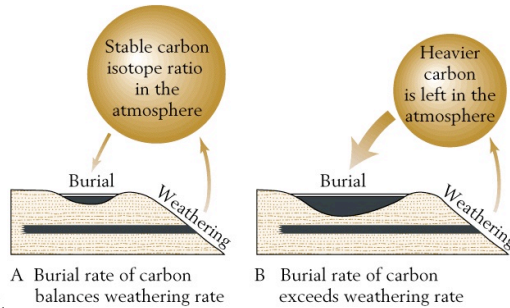
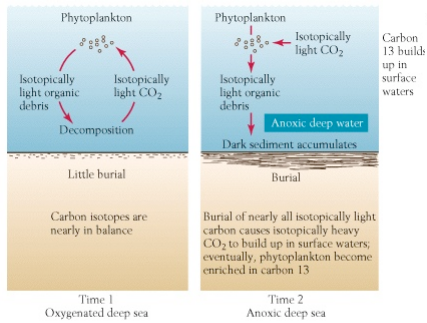
C_{org} burial rate estimated from δ¹³C in CaCO₃



Atmospheric O₂ estimated from C_{org} burial rate

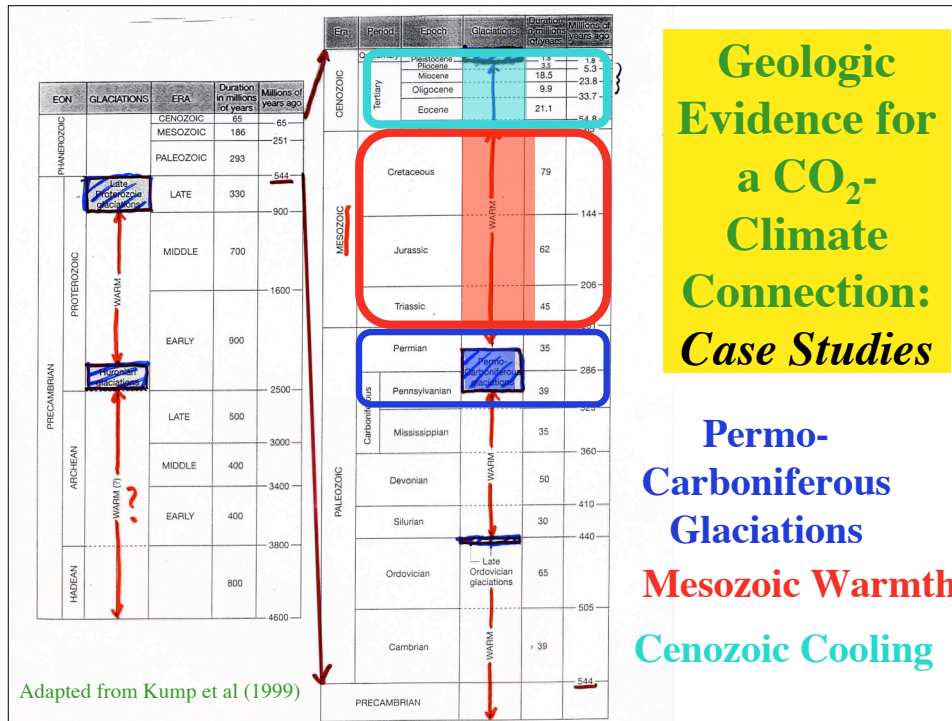
Stanley (2000)

High C_{org} Burial Results in High ¹³C/¹²C in Seawater & CaCO₃



On longer time scales, higher burial rates of C, relative to weathering rates, results in elevated ¹³C/¹²C in atmos/ocean

Stanley (2000)



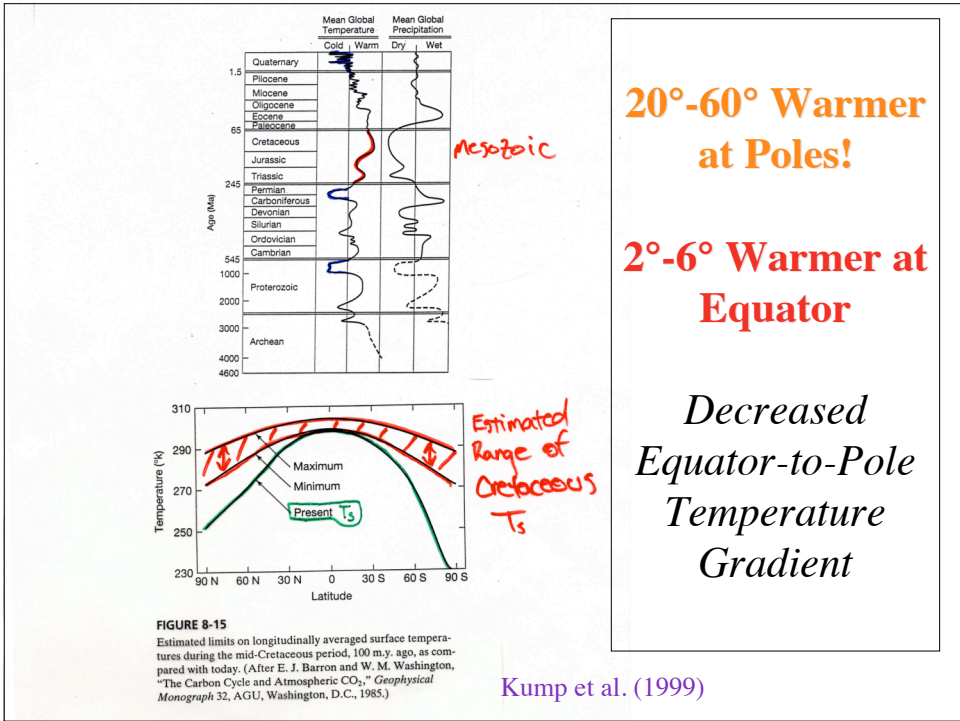
Mesozoic Warmth

Jurassic 220-140 Ma

- Ferns & alligators in Siberia
- Dinosaur bones in AK (N of Arctic Circle)

Cretaceous 140-65 Ma

Stanley (2000)



20°-60° Warmer at Poles!

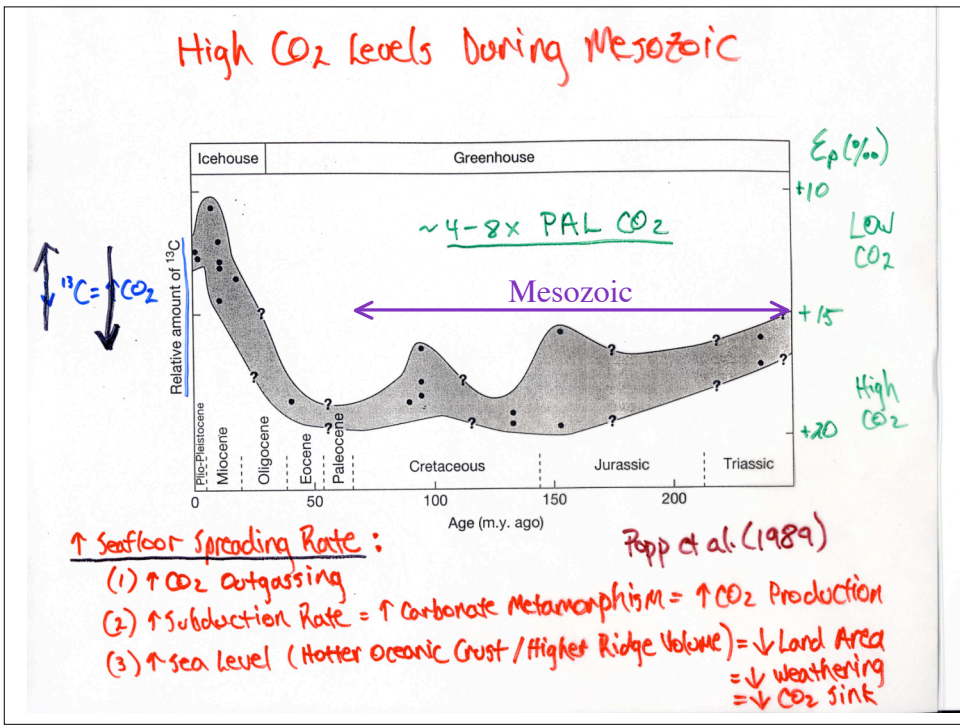
2°-6° Warmer at Equator

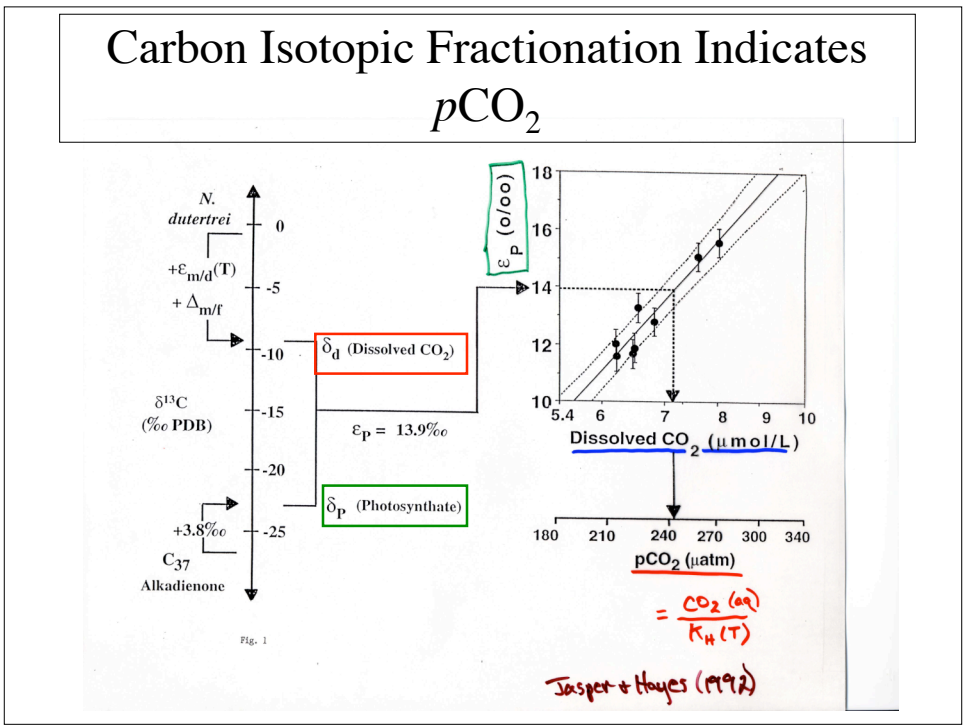
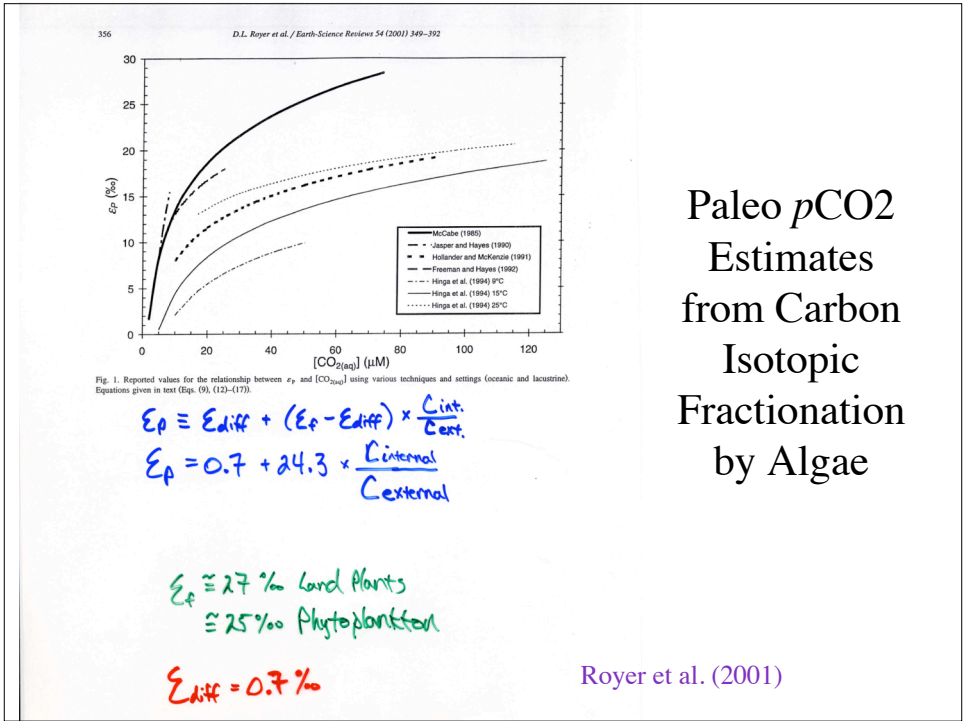
Decreased Equator-to-Pole Temperature Gradient

Mesozoic

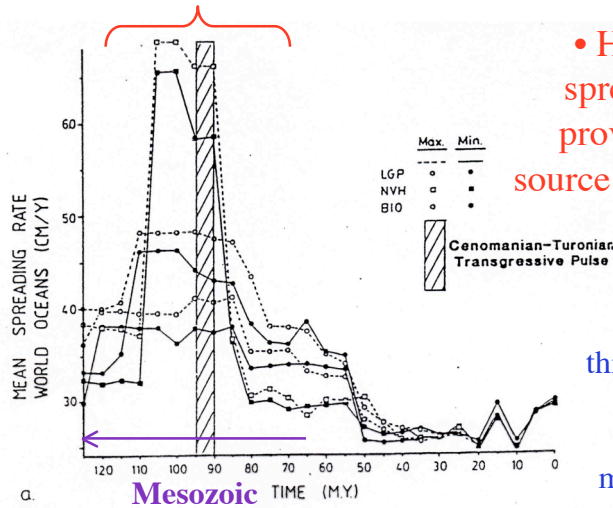
Estimated Range of Cretaceous T_s

Kump et al. (1999)



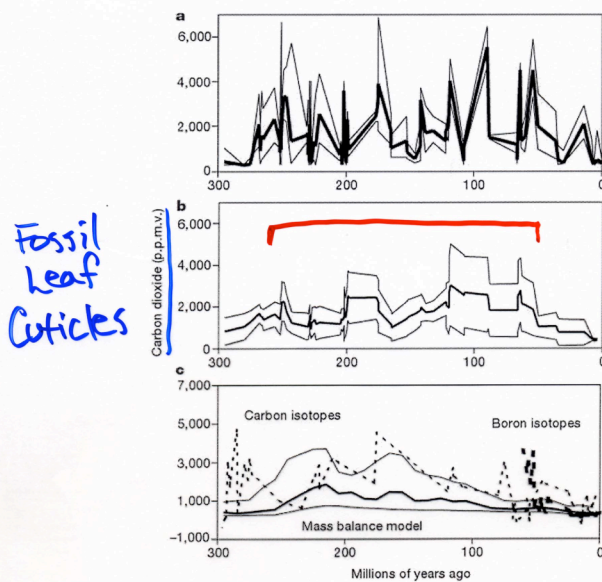


Seafloor Spreading Rates Appear to have Been High in Latter Half of Mesozoic



• High seafloor spreading rates* provide potential source of elevated CO₂

* Determined by thickness of seafloor magnetic stripes between dated magnetic reversals



Fossil leaf Cuticles

Fossil leaf cuticles provide evidence for elevated CO₂ during Mesozoic

3-6 x PAL during Mesozoic

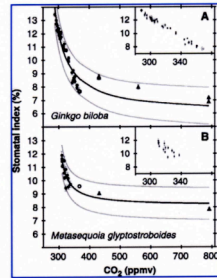
$$SI(\%) = \frac{SD}{(SD+ED)} * 100\%$$

SD= stomatal density
ED=epidermal cell density

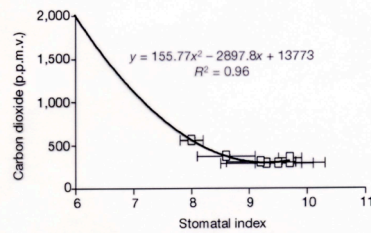
(I.e., the proportion of epidermal cells that are stomata)

Retallack (2001), *Nature*, Vol. 411, pp. 287-290

CO₂ from Leaf Stomatal Indices



Royer et al (2001), *Science*, Vol. 292, pp. 2310-2313



Retallack (2001), *Nature*, Vol. 411, pp. 287-290

Calibrating the Leaf Stomatal “Paleo-barometer”

Extrapolation to high pCO₂ not (yet) supported by data...

Response of stomata to [CO₂] is species-dependent

Limiting SI-derived paleo-CO₂ estimates to times and places when fossilized leaves from extant species exist...

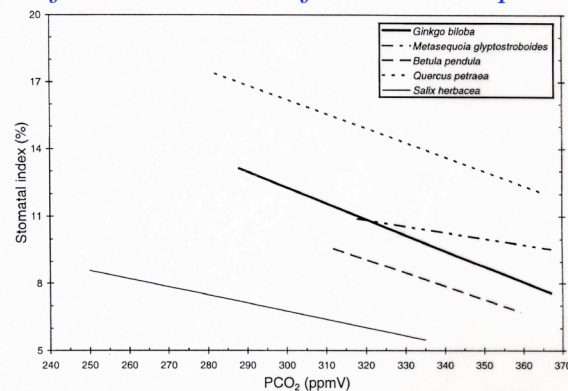
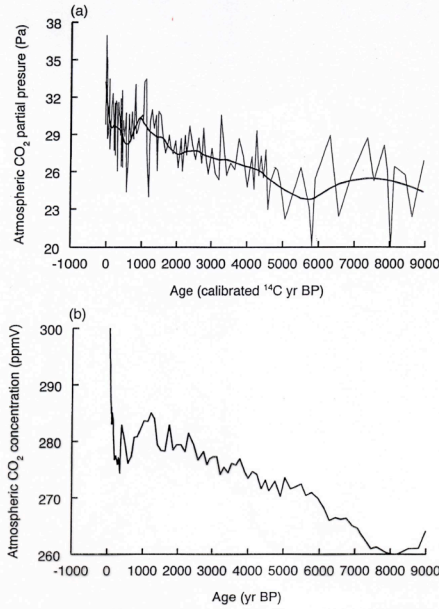


Fig. 9. Stomatal index response of five species to PCO₂. Data compiled from herbarium sheets and altitudinal transects. Sources are as follows: *Ginkgo biloba* and *Metasequoia glyptostroboides* (Royer, unpublished data); *Betula pendula* (Wagner et al., 1996); *Quercus petraea* (Kürschner et al., 1996); *Salix herbacea* (Rundgren and Beerling, 1999).

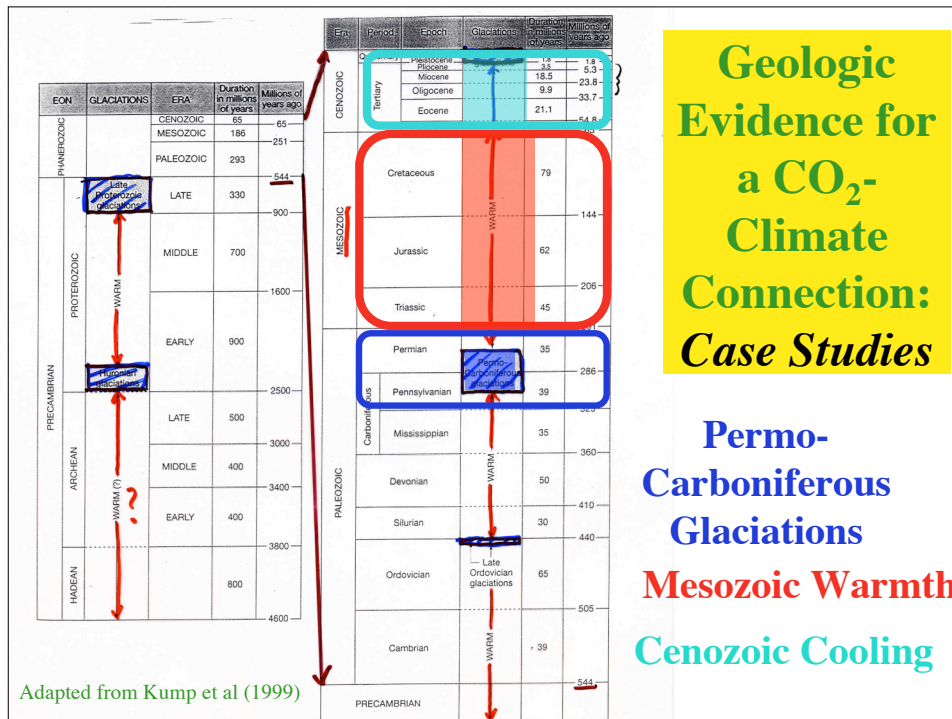
Royer et al. (2001)



**Nevertheless,
calibrations of
the SI appear
accurate for at
least the last 9
kyr**

Royer et al. (2001)

Fig. 12. Holocene reconstructed variations in (a) the partial pressure of atmospheric CO₂ using fossil *Salix herbacea* leaves (after Rundgren and Beerling, 1999) and (b) measurements of atmospheric CO₂ from ice cores (after Indermühle et al., 1999b).

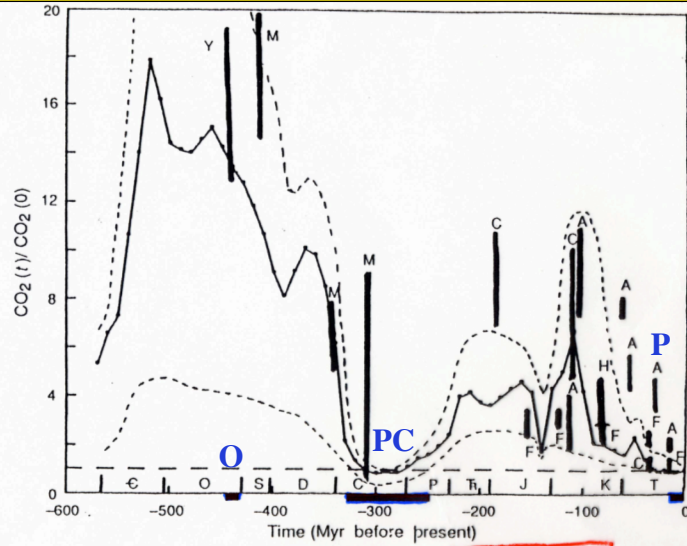


Adapted from Kump et al (1999)

**Geologic
Evidence for
a CO₂-
Climate
Connection:
Case Studies**

**Permo-
Carboniferous
Glaciations
Mesozoic Warmth
Cenozoic Cooling**

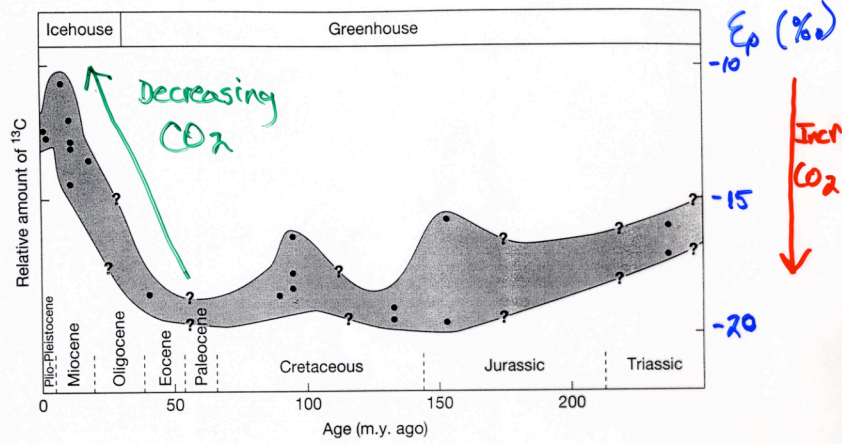
Phanerozoic CO₂ and Climate



Mesozoic

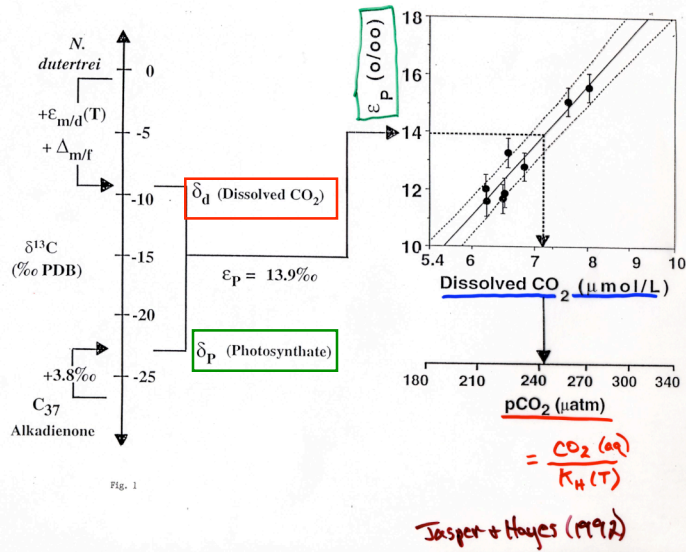
Berner (1992)

Cenozoic CO₂ Decrease

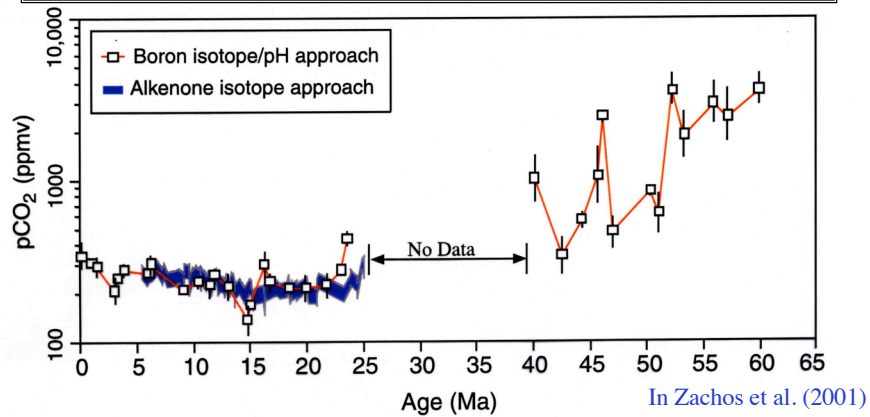


Popp et al. (1989)

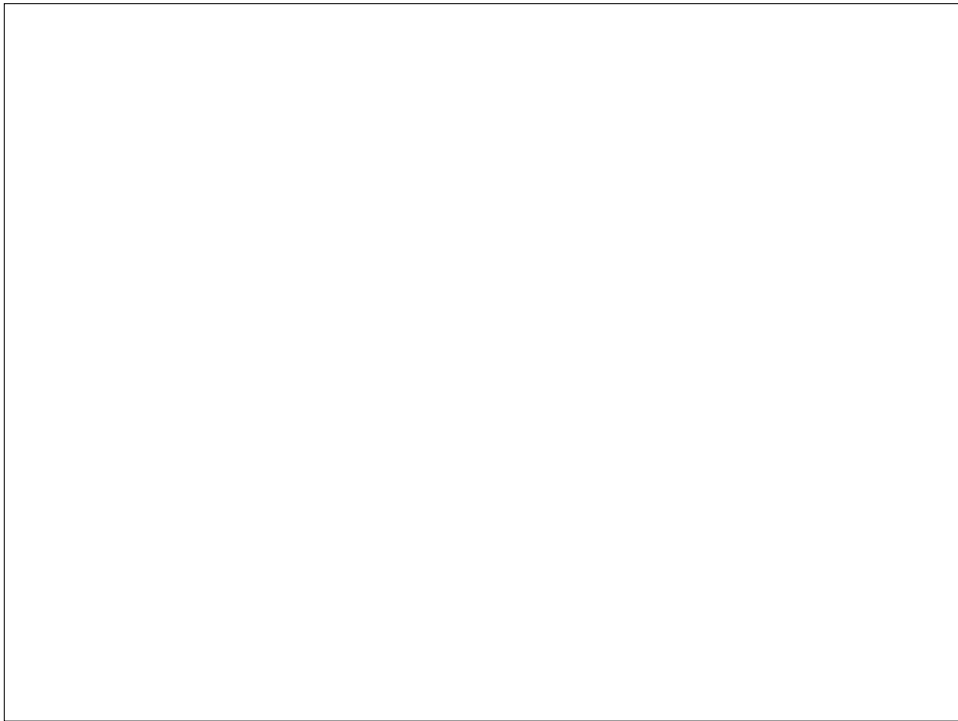
Carbon Isotopic Fractionation Indicates $p\text{CO}_2$



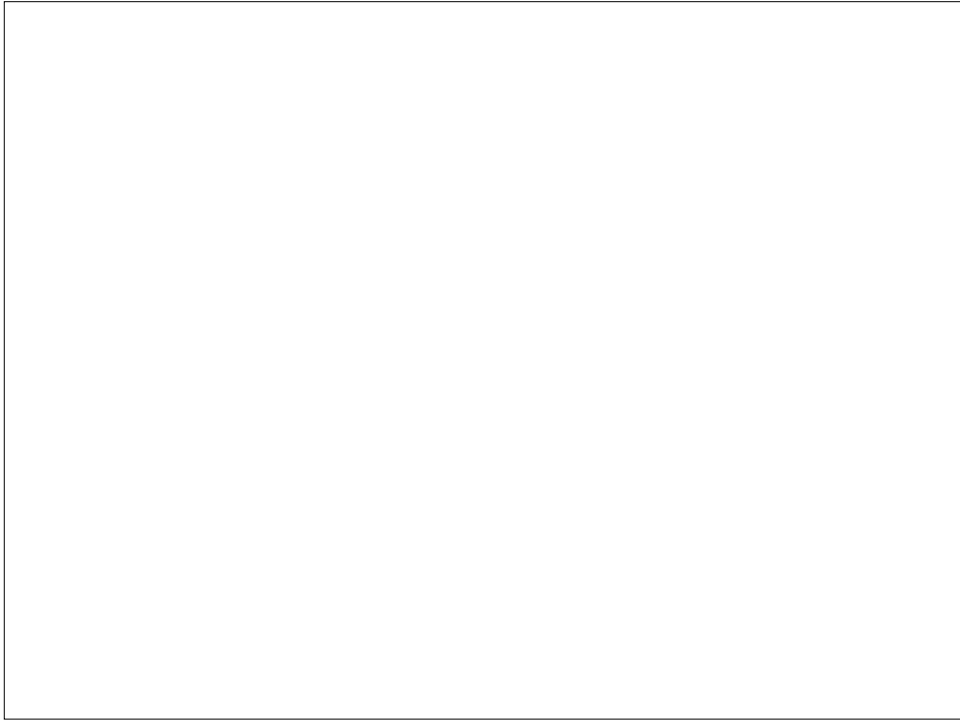
Boron Isotopes in Seawater Also Indicate Large Cenozoic CO_2 Decline



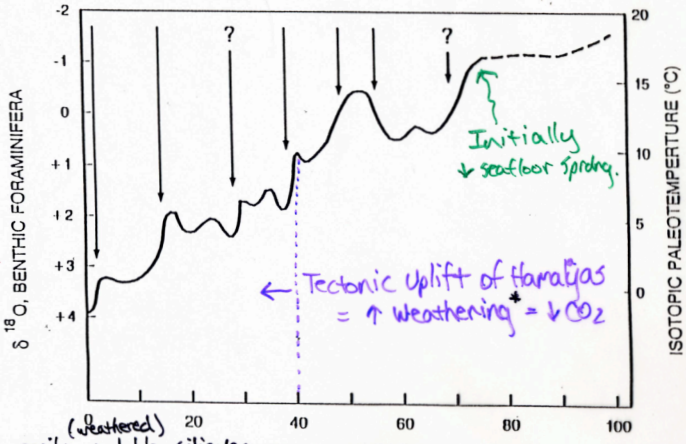
- B in seawater: $\text{B}(\text{OH})_3$, $\text{B}(\text{OH})_4^-$
 - Relative abundance controlled by pH
 - B incorporated into calcite: $\text{B}(\text{OH})_4^-$
 - Strong isotopic fractionation between ^{10}B & ^{11}B :
 ^{10}B = tetrahedral coordination, -19.8‰ relative to ^{11}B
- $\delta^{11}\text{B} = \left[\frac{(^{11}\text{B}/^{10}\text{B})_{\text{sample}}}{(^{11}\text{B}/^{10}\text{B})_{\text{std}}} - 1 \right] \times 1000\text{‰}$



*** Ended Here 11-21-08; Quiz
#3 covers through here ***

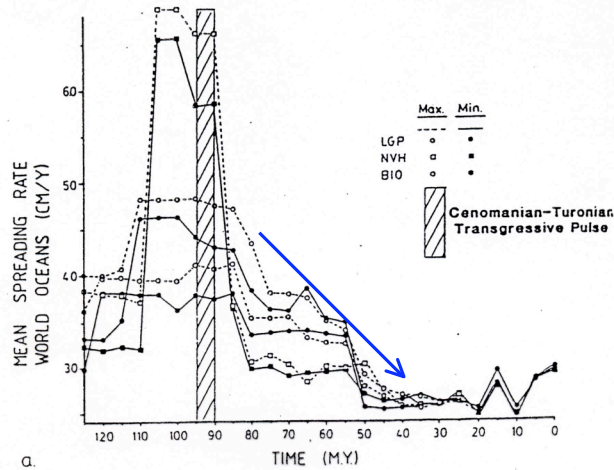


Cenozoic Cooling 80-0 Ma

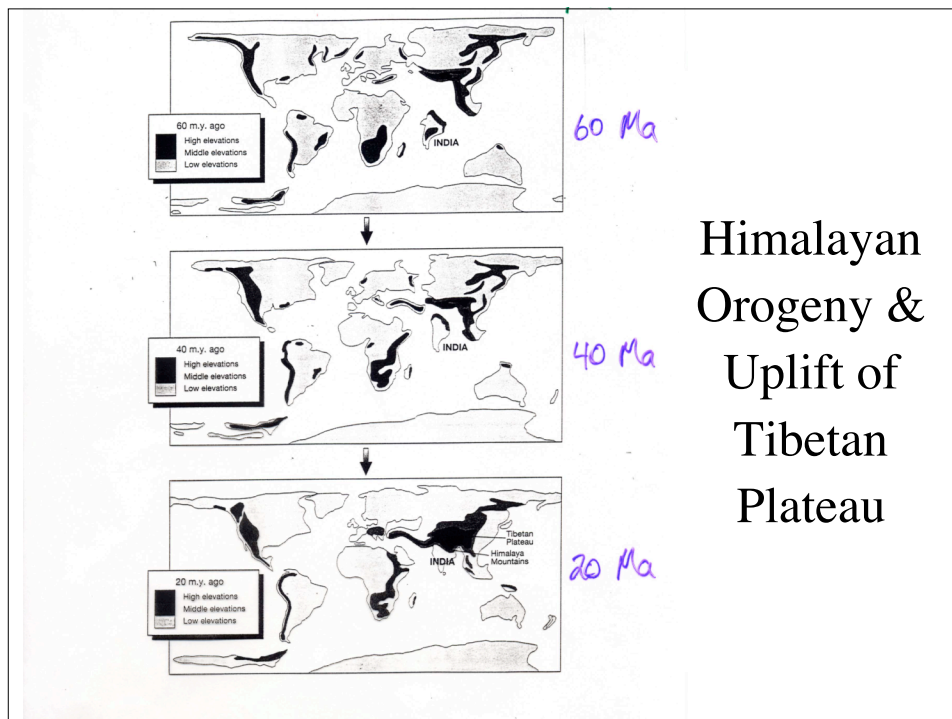


- * Fresh, easily erodable silicates
- * Orographic concentration of rain on mtns. *After Roymo et al. (1988, 1991, 1992)*
- * Steep slopes to rapidly flush weathering products

Declining Seafloor Spreading Rates 80-40 Ma

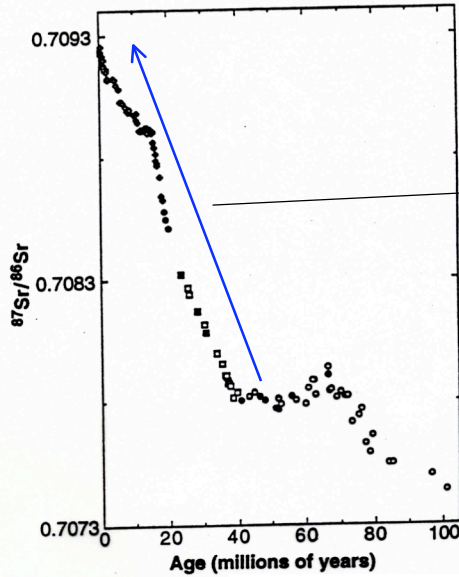


- Declining s.f. spreading rates are consistent with decreasing CO₂ in early Cenozoic



Himalayan Orogeny & Uplift of Tibetan Plateau

Increasing Strontium Isotopic Composition of Seawater During Cenozoic Implies Increasing Weathering Rates



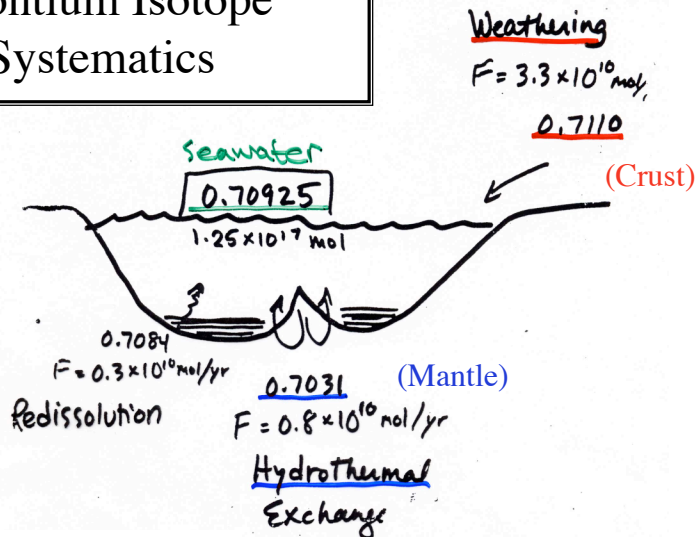
SW $^{87}\text{Sr}/^{86}\text{Sr}$ is balance between:

1. Deep-sea hydrothermal input of non-radiogenic Sr (0.7035)
2. More radiogenic input riverine flux from continental weathering (0.712)

Abyssal carbonate $^{87}\text{Sr}/^{86}\text{Sr}$
 $^{87}\text{Rb} \rightarrow ^{87}\text{Sr}$, $t_{1/2} \sim 48$ Gyr
 • Rb is a lithophilic element that gets concentrated in the crust

DePaolo & Ingram (1985) in Edmond (1992)

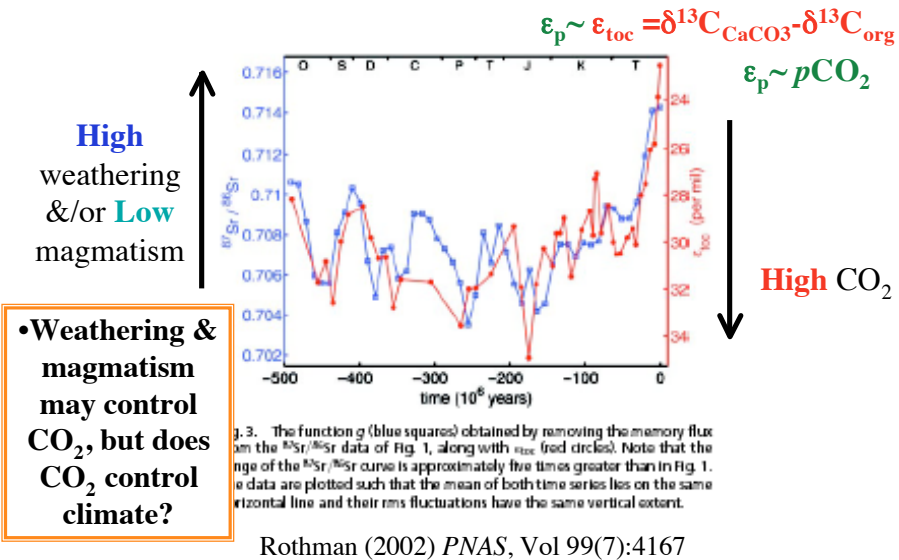
Strontium Isotope Systematics



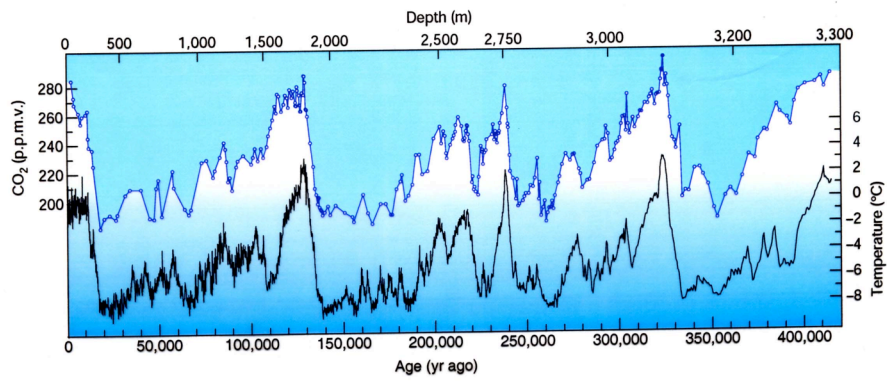
Normal River $^{87}\text{Sr}/^{86}\text{Sr} \sim 0.710$
 Ganges-Brahmaputra $^{87}\text{Sr}/^{86}\text{Sr} \sim 0.8$

Raymo (1998)

Co-Variation of $^{87}\text{Sr}/^{86}\text{Sr}$ & CO_2 through the Phanerozoic



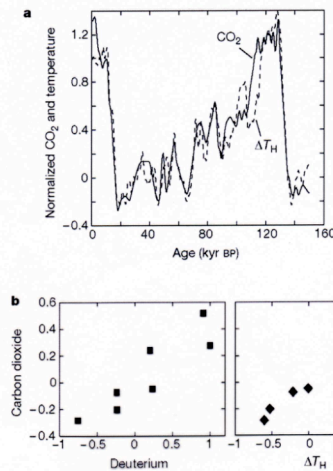
CO_2 During the last 450 kyr from the Vostok, Antarctica Ice Core



Petit et al (1999) in Kump (2002), *Nature*, vol. 419:188-190.

Covariation Between CO₂ and T in Pleistocene

Vostok Ice Core, Central East Antarctica



Cuffey and Vimeux (2001), *Nature*, Vol. 412, pp. 523-527

What caused glacial-interglacial CO₂ variations? (a still-unanswered question!)

Possible Scenario for lower glacial CO₂

- Increased:
Equator-Pole T gradient, Wind strength, Dust flux to ocean, Iron flux to ocean
- 50% of global 1° production occurs in ocean
- Ocean 1° production is limited by iron
- Higher 1° production draws CO₂ out of atmosphere & sequesters it in the deep ocean & sediments
- Colder seawater dissolves more CO₂

letters to nature

2. ... 3. ... 4. ... 5. ... 6. ... 7. ... 8. ... 9. ... 10. ... 11. ... 12. ... 13. ... 14. ... 15. ... 16. ... 17. ... 18. ... 19. ... 20. ... 21. ... 22. ... 23. ...

Correspondence and requests for materials should be addressed to N.E.L. (e-mail: nelson@metu.ca).

Evidence for decoupling of atmospheric CO2 and global climate during the Phanerozoic eon

Jan Veizer*, Veve Godderis† & Louis M. Frappier‡

*Institut für Geologie, Mineralogie und Geophysik, Ruhr Universität, 44780 Bochum, Germany, and †Ottawa-Carleton Geoscience Centre, University of Ottawa, Ottawa, ON K1N 6N5, Canada

Atmospheric carbon dioxide concentrations are believed to drive climate changes from glacial to interglacial modes, although geological and astronomical mechanisms have been invoked as ultimate causes. Additionally, it is unclear whether the changes between cold and warm modes should be regarded as a global phenomenon, affecting tropical and high-latitude temperatures alike, or if they are better described as an expansion and contraction of the latitudinal climate zones, keeping equatorial temperatures approximately constant. Here we present a reconstruction of tropical sea surface temperatures throughout the Phanerozoic eon (the past ~550 Myr) from our database of oxygen isotopes in calcite and argonite shells. The data indicate large oscillations of tropical sea surface temperatures in phase with the cold-warm cycles, thus favouring the idea of climate variability as a global phenomenon. But our data conflict with a temperature reconstruction using an energy balance model that is forced by reconstructed atmospheric carbon dioxide concentrations. The results can be reconciled if atmospheric carbon dioxide concentrations were not the principal driver of climate variability on geological timescales for at least one-third of the Phanerozoic eon, or if the reconstructed carbon dioxide concentrations are not reliable.

Calculated partial pressures of CO2 in the atmosphere (pCO2) are indeed relatively low for the Permian-Carboniferous and Cretaceous icehouse episodes, times of predominantly cold climates lasting tens of millions of years, but for the other two Phanerozoic icehouses—the late Ordovician-Carboniferous and the late Permian-Cretaceous—all global biogeochemical models predict high pCO2 levels. In an attempt to resolve this discrepancy, particularly for the late Ordovician glaciation(s), theoretical models advocating the development of permanent high-latitude ice sheets at more than 10 times present-day CO2 levels have been proposed. As an alternative, we present here experimental evidence that suggests large variations in tropical sea surface temperatures (SSTs) up to 9 °C between the peaks of greenhouse/icehouse modes. The testing of model predictions on Phanerozoic timescales has been hampered by the lack of high-resolution isotope databases for ancient sea water, as reflected in (bio)chemical sediments. This has been particularly the case for oxygen isotopes, where the depletion in 18O for progressively older sediments was mostly considered to be a product of post-depositional diagenetic overprint. However, new databases have been published recently—based on ~400 low-Mg calcitic and 125 argonitic shells—for 813, 814, 815 and 816Mg, establishing the baseline for Phanerozoic 818O (Fig. 1 in ref. 17). Most studied samples originate from the photic zone of palaeotropical seas (20°S–30°N). The entire datasets are available at http://www.science.ottawa.ca/geology/isotope_data. Reference 17, because of the huge number of measurements, dealt only with the documentation of data and their quality, and with the argument for the primary nature of the 818O record. The secular trend for the 818O values of Phanerozoic carbonates, Fig. 13 in ref. 17, consists of a long-term rising linear trend that exceeds the duration of planetary greenhouse/icehouse modes. This trend is tectonically controlled, a proposition supported by the strong correlation of 818O with the 87Sr/86Sr signal for the Phanerozoic sea water (Figs 16 and 17 in ref. 17). Sr isotopes are a proxy for tectonic tectonic processes, because seawater 87Sr/86Sr is controlled principally by inputs of Sr from rivers (resulting of Sr-enriched continental crust) and from hydrothermal circulation cells at mid-ocean ridges (interaction with 87Sr-depleted basalt). Such long-term tectonic signals have to be subtracted from the superimposed higher-order oscillations before any discussion of climatic consequences, and we therefore detrended the data by removing the least-squares linear fit. The first-order 818O oscillations around the least-squares fit correlate well with the palaeoclimate as established from sedimentological criteria. The icehouses usually coincide with 18O-enriched values and greenhouse with 18O-depleted values (Fig. 1). We propose therefore that the Phanerozoic 818O oscillations reflect variations in SSTs. Future improvements on the Phanerozoic database may result in amelioration of the amplitude, or in partial temporal shifts of some of the peaks. This is particularly the case for the Neoproterozoic interval, where the timing means is forced to higher values by the inclusion of some isotopically heavy planktonic

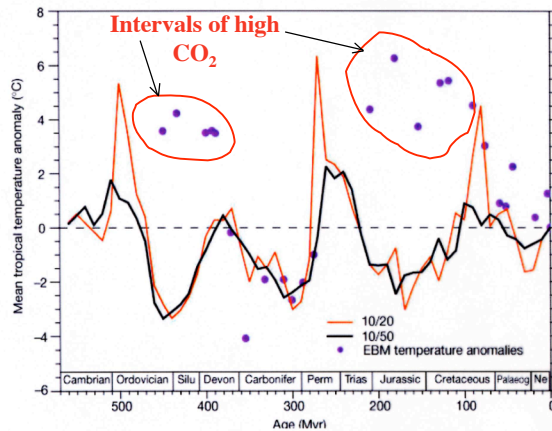
While a large and growing body of evidence indicates that CO2 and climate co-vary, there is some indication that the two may not be closely linked at all times....

(& it is always important to remember that correlation does not always mean causation)

*** Ended Here - 12/1/08 ***

Cool Tropics - High CO₂ (?)

Model-Data SST Comparison



Tropical SST anomaly (Data)

- Assumes 2‰ of 3-5‰ δ¹⁸O range due to ice volume (2x present ice volume in “icehouse”; No ice in “greenhouse”).
- Leaves ~2‰, or ~9°C of SST change

Simple E Balance Model

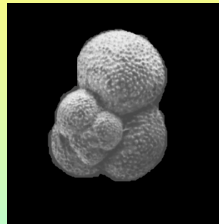
- CO₂ (Berner, 1992)
- Solar constant increasing by 5% over Phanerozoic

$$T_s - \Delta T_g = T_{\text{eff}}$$

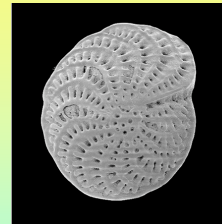
$$\sigma T_{\text{eff}}^4 = S/4 * (1-A)$$

Veizer et al. (2000), *Nature*, Vol. 408, pp. 698-701
(or diagenetic alteration of CaCO₃?)

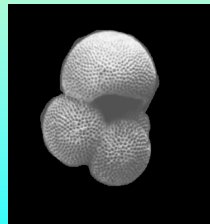
Seawater Temperatures from Oxygen Isotopes in Foraminifera



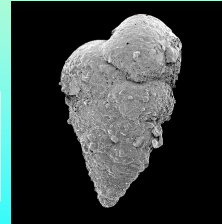
Globigerina bulloides



Elphidium macellum



Globigerinoides sacculifer



Siphotextularia concava

Natural Abundances
¹⁶O = 99.756%
¹⁷O = 0.039
¹⁸O = 0.205

$$\delta^{18}\text{O} = \left[\frac{(^{18}\text{O}/^{16}\text{O})_{\text{sample}}}{(^{18}\text{O}/^{16}\text{O})_{\text{standard}}} - 1 \right] \times 1000\text{‰}$$

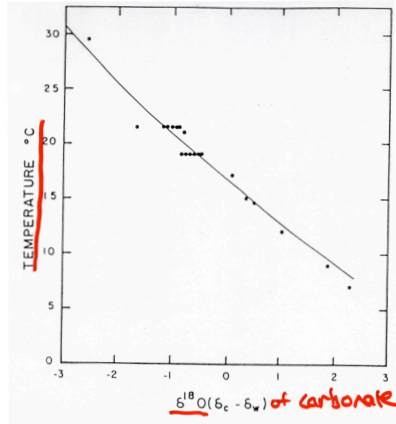
Planktonic Foraminifera

Benthic Foraminifera

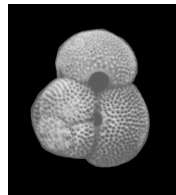
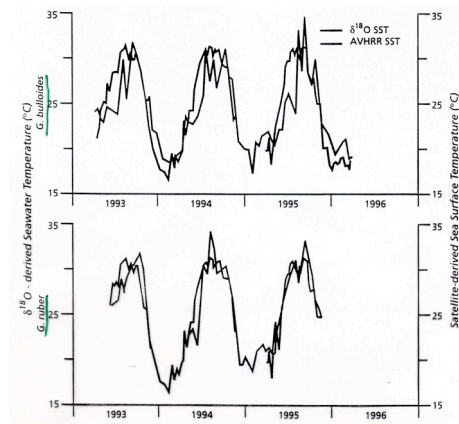
SEM Images: <http://www.ucl.ac.uk/GeolSci/micropal/foram.html>

d18O_Faunal-Floral_SST_Module_3, 10/11/06 7:50 pm

T-Dependent $^{18}\text{O}/^{16}\text{O}$ Fractionation Occurs During Calcification



Epstein et al. (1953) *Geological Society of America Bulletin*, 64, 1315-1326



Globigerinoides ruber



Globigerina bulloides

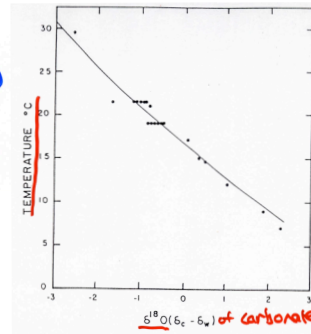
SEM images: <http://www.ucl.ac.uk/GeolSci/micropal/foram.html>

But T is not the only variable that effects $\delta^{18}\text{O}$ values of CaCO_3 ... Must also consider water $\delta^{18}\text{O}$



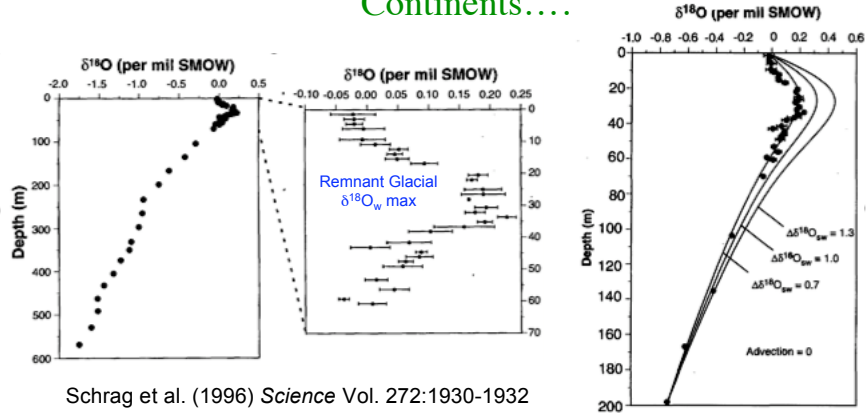
$$T = 16.9 - 4.2 (\delta^{18}\text{O}_c - \delta^{18}\text{O}_w)$$

- Water $\delta^{18}\text{O}$ is dependant upon other key climate variables:



$$\delta^{18}\text{O}_w = f(\text{precipitation, evaporation, runoff, global ice volume})$$

The Whole Ocean $\delta^{18}\text{O}$ Changes with Volume of Ice on Continents....



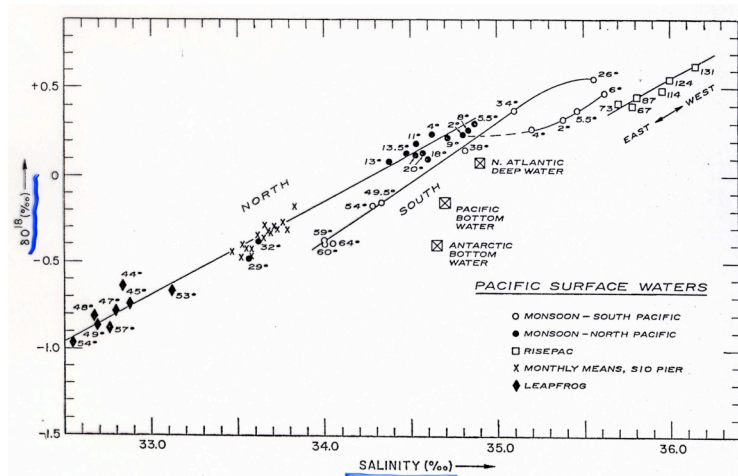
Schrag et al. (1996) *Science* Vol. 272:1930-1932

- Apply 1-D advection-diffusion model to isotope data to determine that glacial ocean was 0.8-1‰ enriched in ^{18}O relative to the Holocene period.

$$dC/dt = D_s d^2C/dz^2 - w dC/dt$$

- C = concentration of ^{18}O or ^{16}O
- D_s = diffusion coefficient of ^{18}O or ^{16}O
- w = advection rate

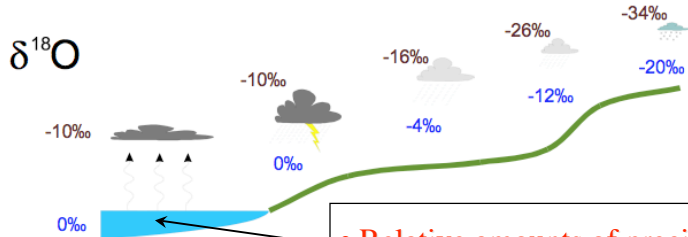
$\delta^{18}\text{O}$ SST Problem # 2: Seawater $\delta^{18}\text{O}$ Varies with Salinity -- Why?



Craig & Gordon (1965) In: *Proceedings of a Conference on Stable Isotopes in Oceanographic Studies and Paleotemperatures* (Ed. by E. Tongioli), pp. 9-130. CNR-Laboratorio di Geologia Nucleare, Pisa.

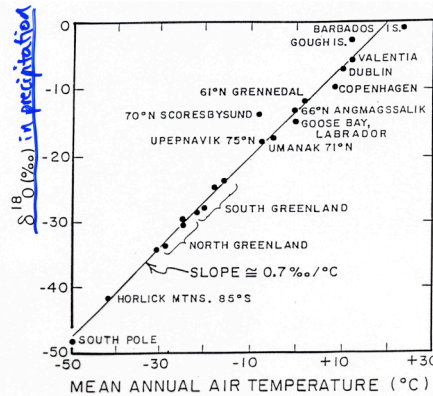
Rainout and Rayleigh Distillation

Warm  **Cold**
 Low elevation Low latitude High elevation High latitude



• Relative amounts of precipitation & evaporation, plus storm tracks, humidity, winds, seasonality, etc. all influence seawater $\delta^{18}\text{O}$ values!

Schematic from Clark & Aravena



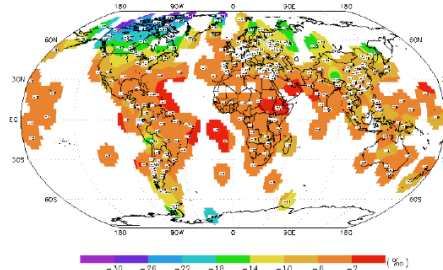
• Precipitation $\delta^{18}\text{O}$ values vary with latitude & altitude

• Runoff from melting snow & ice is highly depleted in ^{18}O

• H_2^{18}O has 1% lower vapor pressure

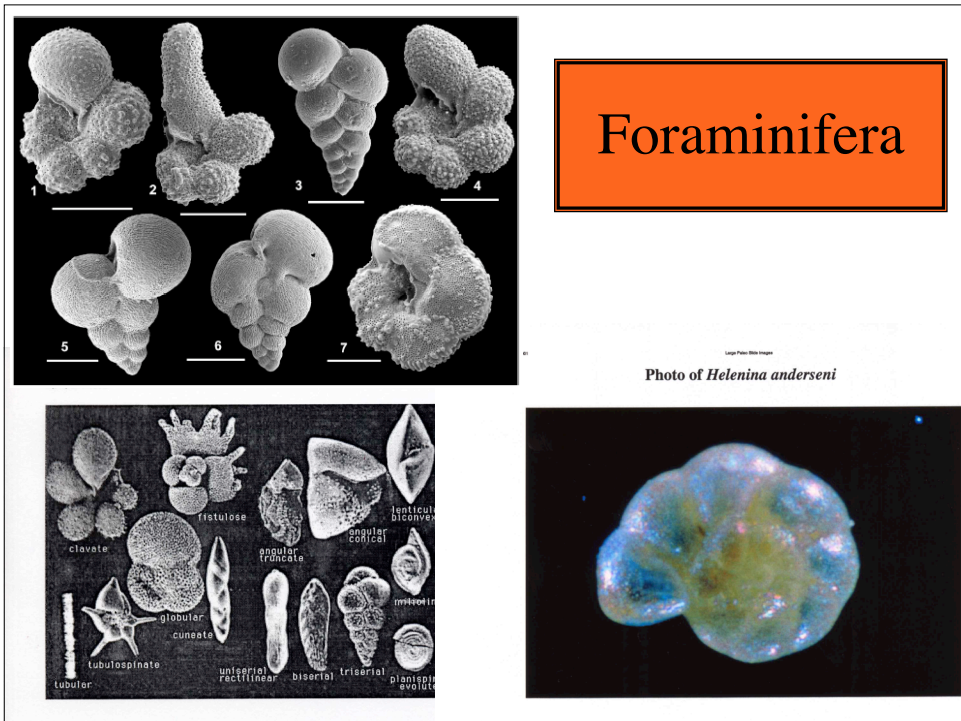
Dansgaard (1964) *Tellus*, 16: 436-447

Weighted Annual $\delta^{18}\text{O}$ with Station Data

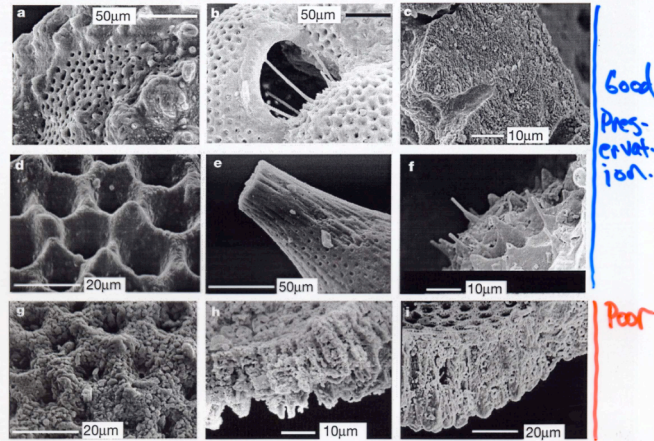


<http://isohis.iaea.org/>

$\delta^{18}\text{O}$ -derived SST
Problem #3:
Diagenetic Alteration of
 $^{18}\text{O}/^{16}\text{O}$ in CaCO_3



Recrystallization of Foramin Calcite

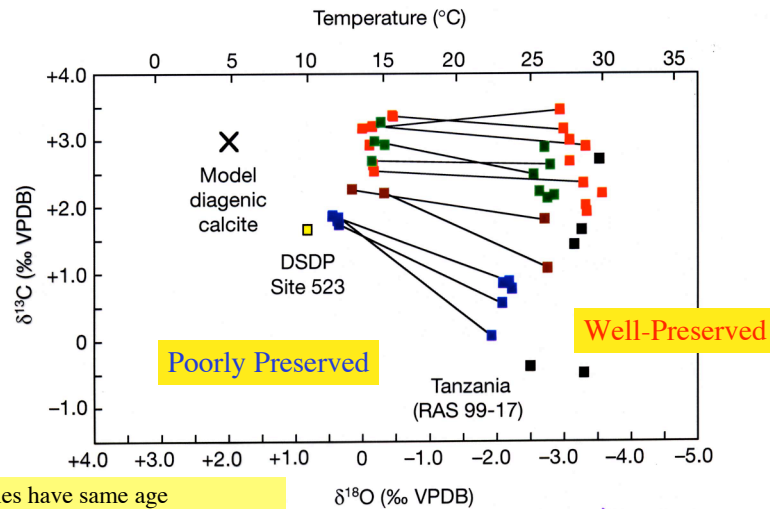


Good Pres-
ervation.

Poor

Pearson et al. (2001),
Nature, 413: 481-487

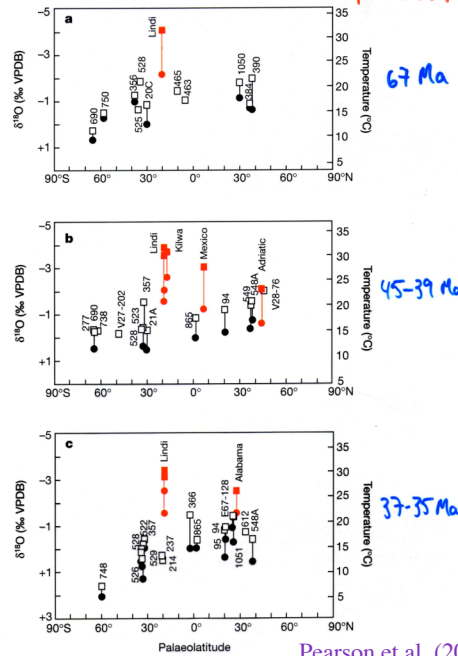
Large Effect of Diagenesis Makes T Estimates Biased to Cold



- Samples have same age
- Lines connect same species of foraminifera

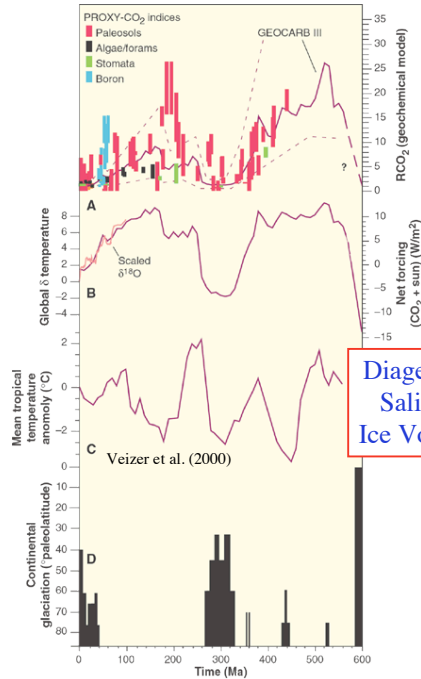
Pearson et al. (2001) *Nature* Vol. 413: 481-487.

Well-Preserved Forams Indicate ↑ Tropical SST (During Eocene)



Well-Preserved Fossils are Essential!

CO₂ & Climate



Diagenesis?
Salinity?
Ice Volume?

Records of change. (A) Comparison of CO₂ concentrations from the GEOCARB III model with a compilation of proxy-CO₂ evidence (vertical bars). Dashed lines: estimates of uncertainty in the geochemical model values. Solid line: conjectured extension to the late Neoproterozoic (about 590 to 600 Ma). RCO₂, ratio of CO₂ levels with respect to the present (300 parts per million). (B) Radiative forcing for CO₂ corrected for changing luminosity after adjusting for an assumed 30% planetary albedo. Deep-sea oxygen isotope data over the past 100 Ma have been scaled to global temperature variations. (C) Oxygen isotope-based low-latitude paleotemperatures. (D) Glaciological data for continental-scale ice sheets based on many sources.

Crowley & Berner (2002) *Science*, Vol. 292:870.

However, even with well-preserved foraminifera, Cretaceous warmth may have commenced *after* large (inferred) CO₂ emission by seafloor spreading...

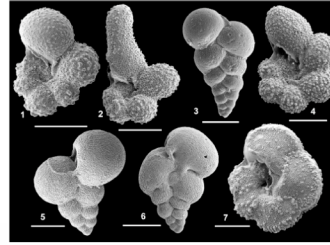
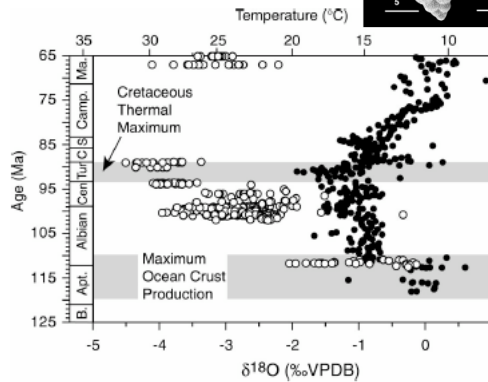


Figure 3. Comparison of Cretaceous $\delta^{18}\text{O}$ -temperature records indicates 20–40 m.y. mismatch between peak Cretaceous-Cenozoic global warmth (Cretaceous thermal maximum) and peak Cretaceous-Cenozoic tectonic CO₂ production inferred from ocean-crust cycling (Larson, 1991). Glassy planktic foraminifera (open symbols) from low-latitude western tropical Atlantic (plus Maastrichtian data from Tanzania and Gulf Coast) vs. bulk carbonate (solid symbols) from high-latitude Southern Indian Ocean (Clarke and Jenkyns, 1999; Erbacher et al., 2001; Wilson and Norris, 2001; Pearson et al., 2001; Norris et al., 2002). All temperatures calculated in same way as conservative temperatures in Figure 2 and would be 3–6 °C higher if modern latitudinal trends in $\delta\omega$ (global mean Cretaceous seawater) were applied (see text).



Wilson et al. *Geology* (2002)

Other Evidence for Weak CO₂ - Climate Connection during Phanerozoic

$$\epsilon_p \sim p\text{CO}_2$$

$$\epsilon_p \sim \epsilon_{\text{toc}} = \delta^{13}\text{C}_{\text{CaCO}_3} - \delta^{13}\text{C}_{\text{org}}$$

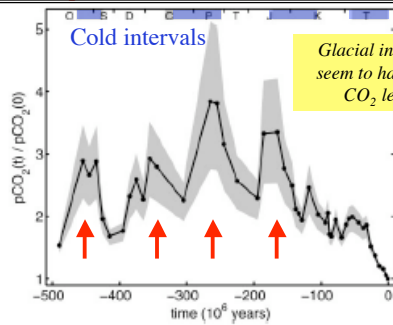
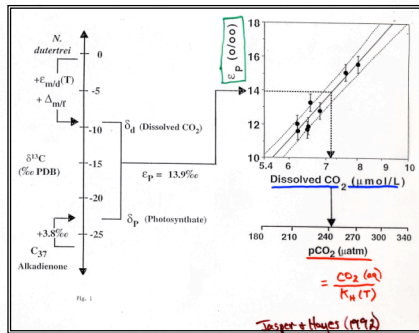
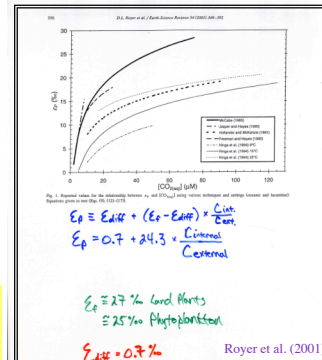


Fig. 4. Fluctuations of $p\text{CO}_2$ for the last 500 My, normalized by the estimate of $p\text{CO}_2$ obtained from the most recent value of ζ . The solid line is obtained from Eq. 12 by using $\zeta_0 = 36\%$. The lower and upper limits of the gray area surrounding the $p\text{CO}_2$ curve result from $\zeta_0 = 38$ and 35% , respectively. The gray bars at the top correspond to periods when Earth's climate was relatively cool; the white spaces between them correspond to warm modes (18).

Rothman (2002) *PNAS*



But different CO₂ proxies lead to different results....

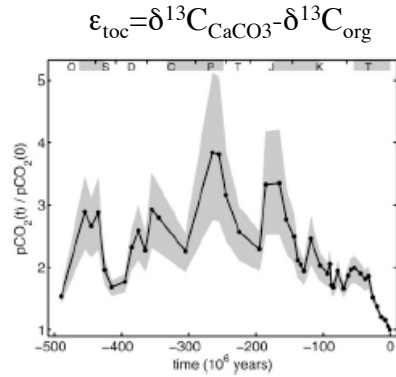


Fig. 4. Fluctuations of $p\text{CO}_2$ for the last 500 Myr, normalized by the estimate of $p\text{CO}_2$ obtained from the most recent value of ϵ . The solid line is obtained from Eq. 12 by using $\epsilon_{\text{org}} = 36\text{‰}$. The lower and upper limits of the gray area surrounding the $p\text{CO}_2$ curve result from $\epsilon_{\text{org}} = 38$ and 35‰ , respectively. The gray bars at the top correspond to periods when Earth's climate was relatively cool; the white spaces between them correspond to warm modes (18).

Rothman (2002)

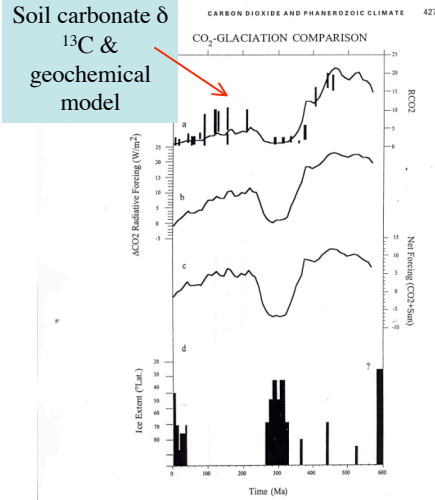
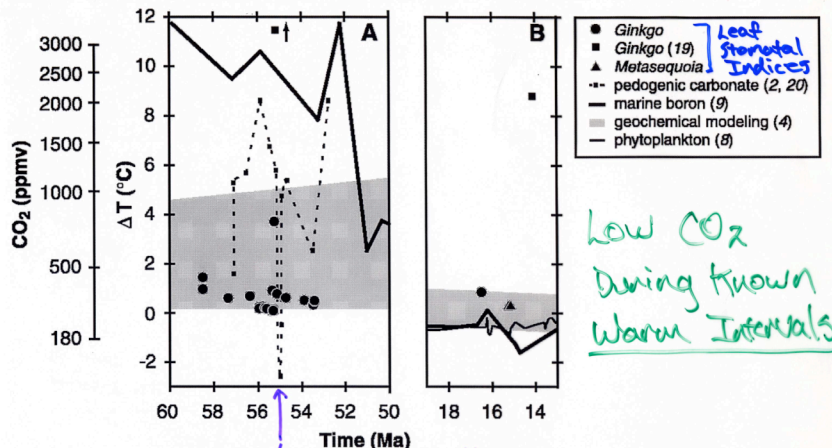


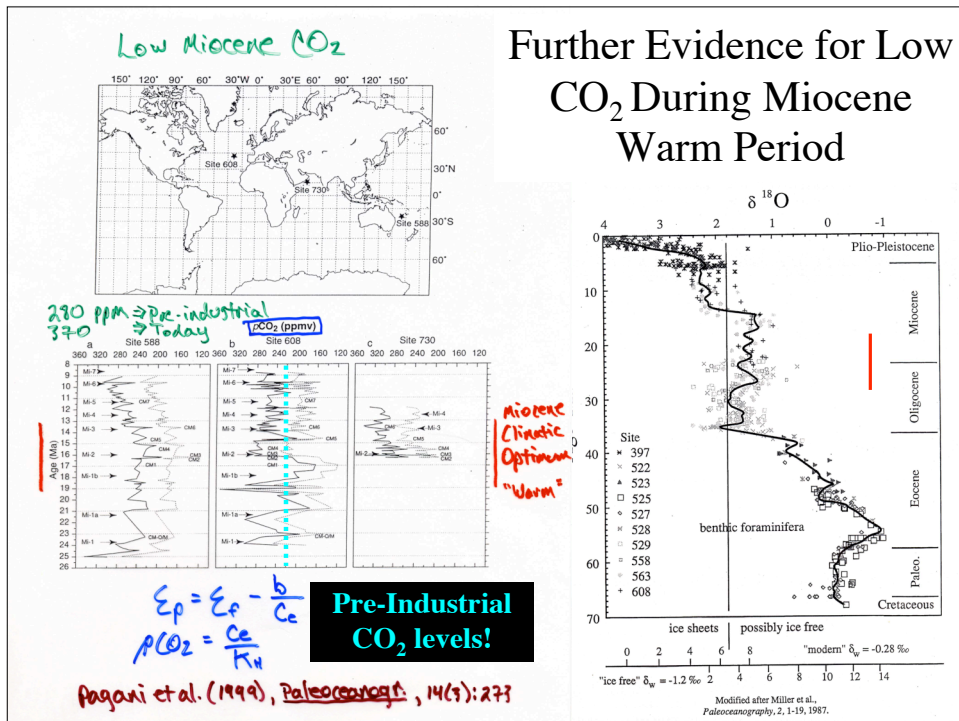
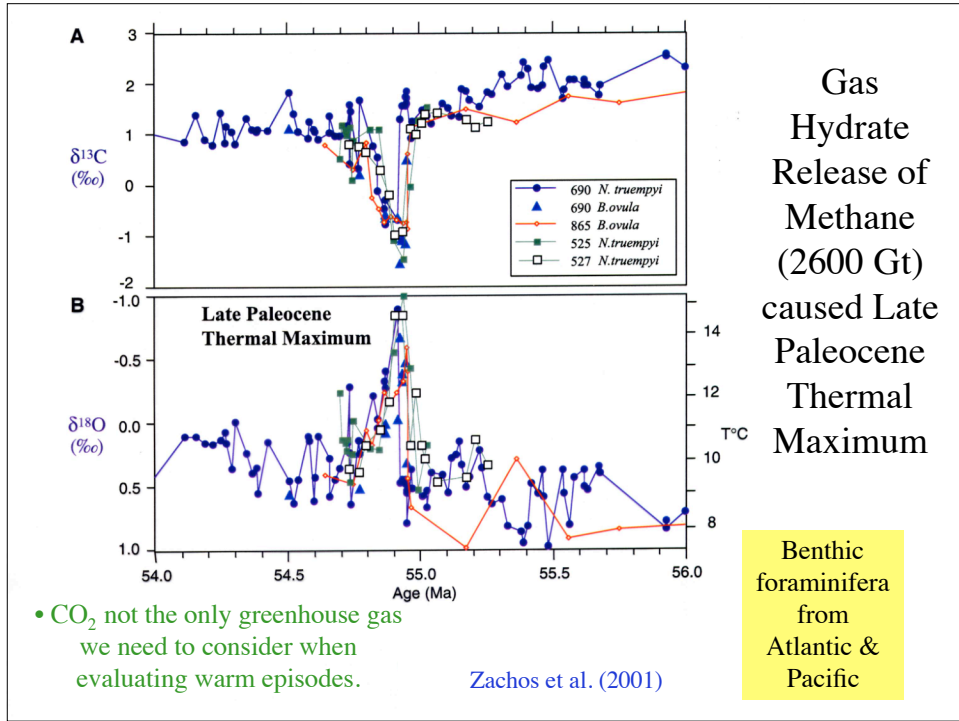
Figure 14.1. (a) Comparison of CO_2 concentrations from a geochemical model (Berner, 1994) with a compilation (Berner, 1997) of proxy CO_2 estimates (vertical bars). CO_2 (b) and solar relative (c) forcing effects (W m^{-2}) as discussed in the text. Glaciological evidence for continental-scale glaciation (d) from Crowley (1998), which in turn was modified from a compilation from many sources. See text for further discussion.

Crowley (2000)

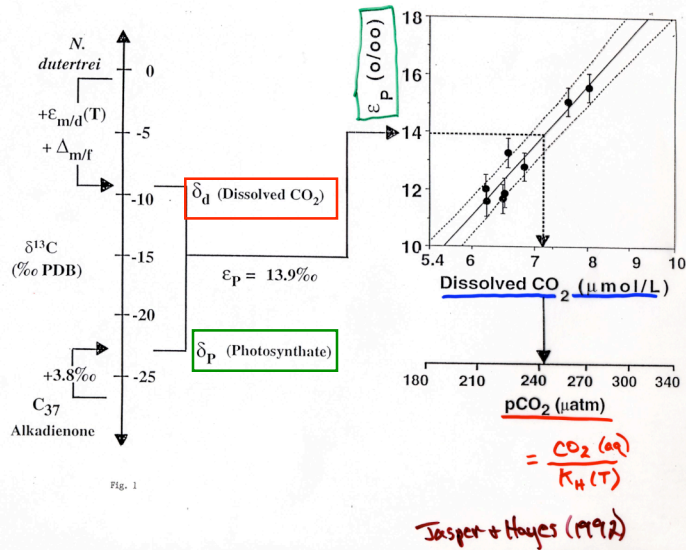
Other evidence for Low CO₂ During Known Warm Periods



Royer, et al. (2001)
Science, Vol. 292, p. 230

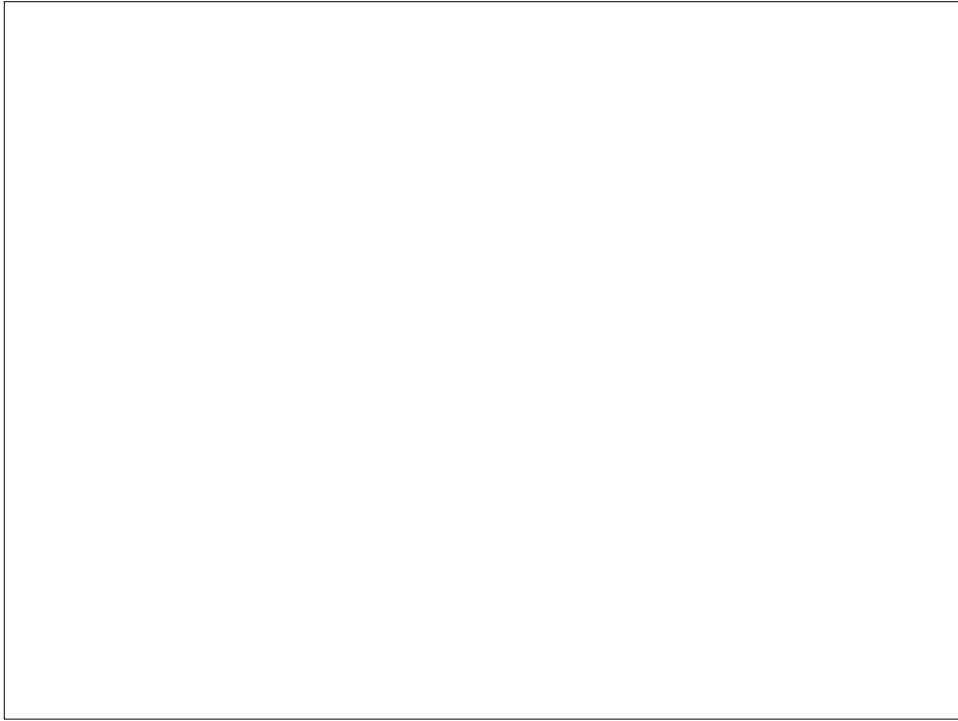


Carbon Isotopic Fractionation Indicates $p\text{CO}_2$

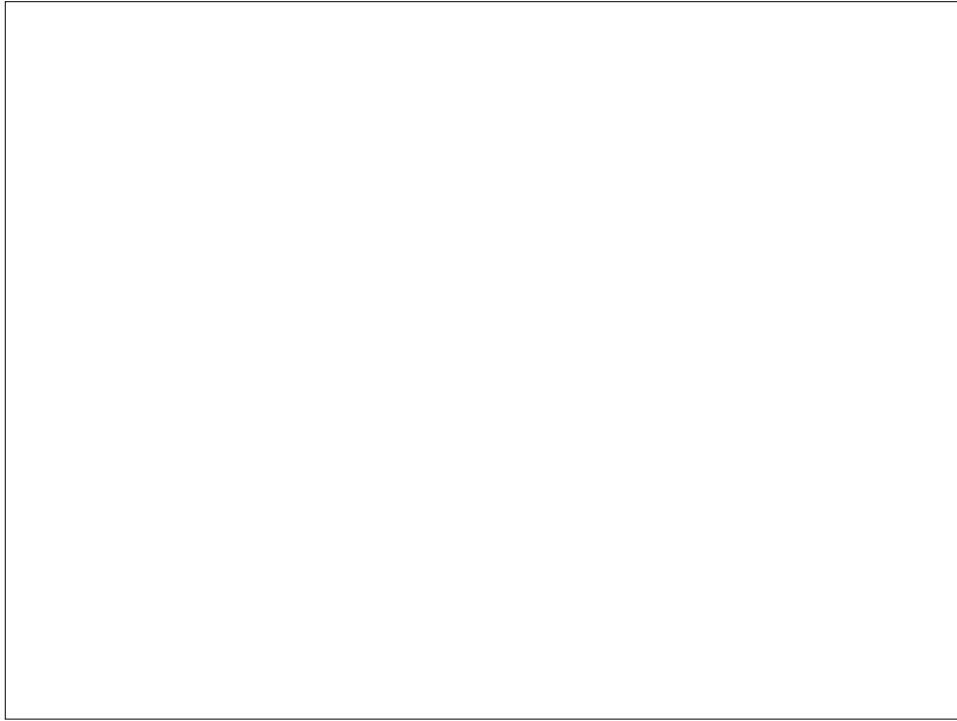


Substantial evidence exists for a strong link between CO_2 & climate on a variety of timescales....
With some notable exceptions!

Additional paleoclimate reconstructions & numerical model simulations are necessary. But the biggest (non-controlled) experiment ever attempted is now underway...



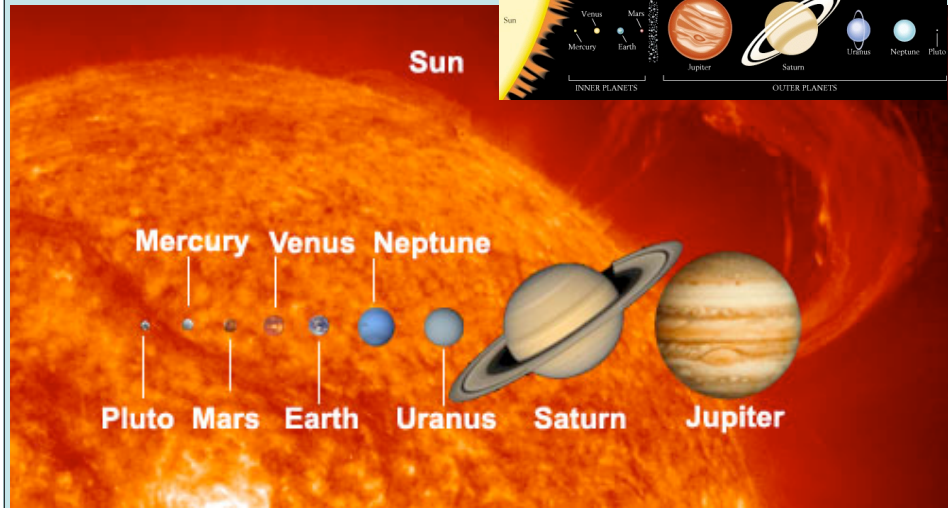
***** Ended Here - 12/3/08 *****



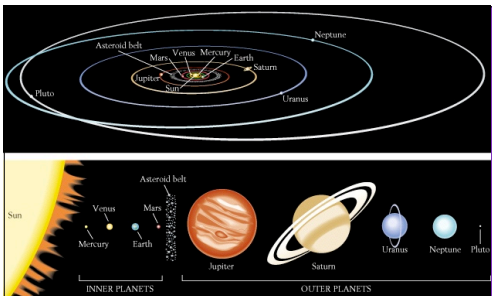
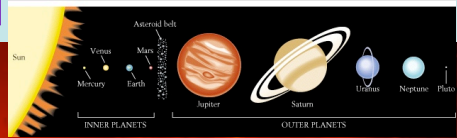
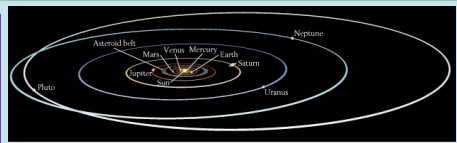
**External
Influences
on
Climate**



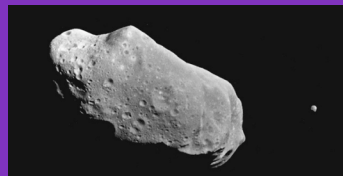
The Sun & Planets to Scale



NASA-JPL



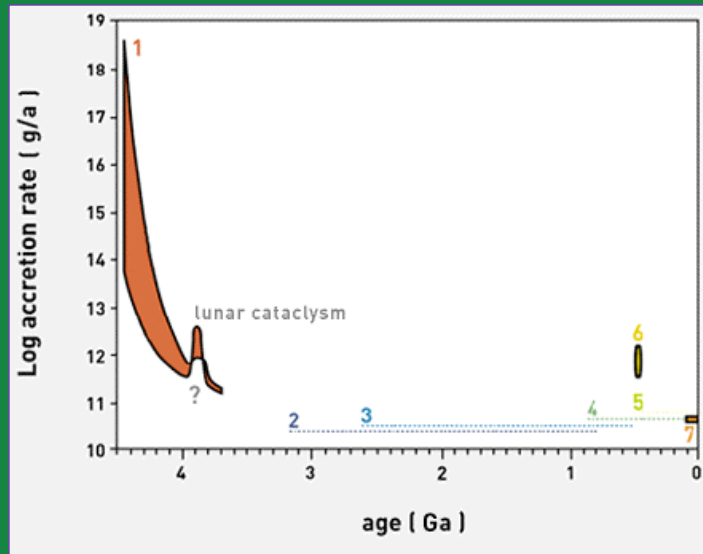
The Asteroid Belt



- A relic of the accretion process. A failed planet.
- Gravitational influence of Jupiter accelerates material in that location to high velocity.
- High-velocity collisions between chunks of rock shatter them.
- The sizes of the largest asteroids are decreasing with time.

Total mass (Earth = 1)	0.001
Number of objects > 1 km	~100,000
Number of objects > 250 km	~12
Distance from Sun	2-4 AU
Width of asteroid belt (million km)	180

Earth Accretion Rate Through Time

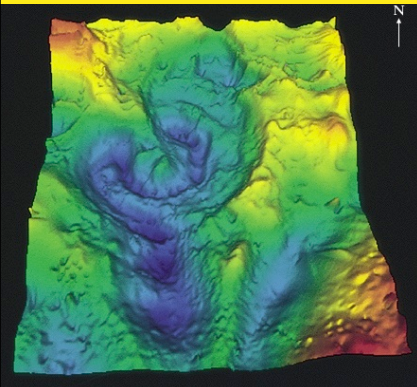


Schmitz et al., (1997) *Science*, Vol. 278: 88-90, and references therein.
<http://www.whoi.edu/science/MCG/pge/project4.html>

Accretion continues...

Chicxulub Crater, Gulf of Mexico

- 200 km crater
- 10-km impactor
- 65 Myr BP
- Extinction of 75% of all species!

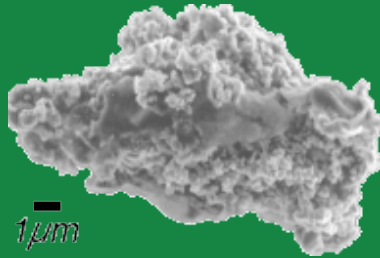


Meteor (Barringer) Crater, Arizona

- 1 km diam. Crater
- 40-m diam Fe-meteorite
- 50 kyr BP
- 300,000 Mton
- 15 km/s

<http://www.gi.alaska.edu/rem sense/features/impactcrater/imagexplain.htm>

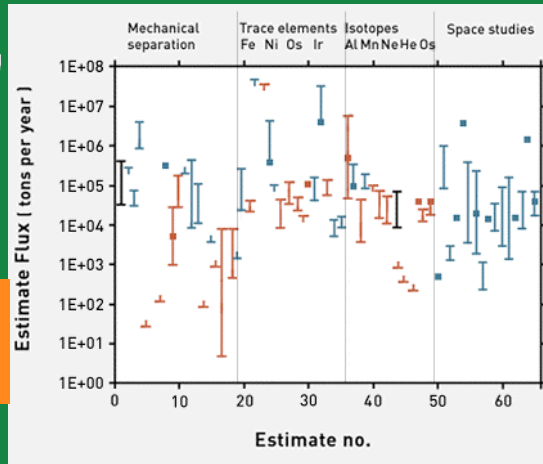
Interplanetary Dust Accumulation



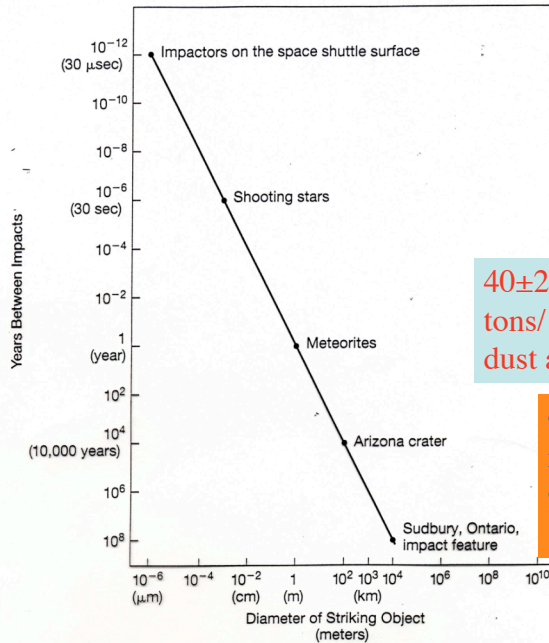
1 μm

<http://presolar.wustl.edu/work/idp.html>

$40 \pm 20 \times 10^4$ metric tons/ yr
(40×10^{10} g) interplanetary
dust accretes every yr!



<http://www.whoi.edu/science/MCG/pgc/project4.html>



Size - Frequency Distribution of Impacts

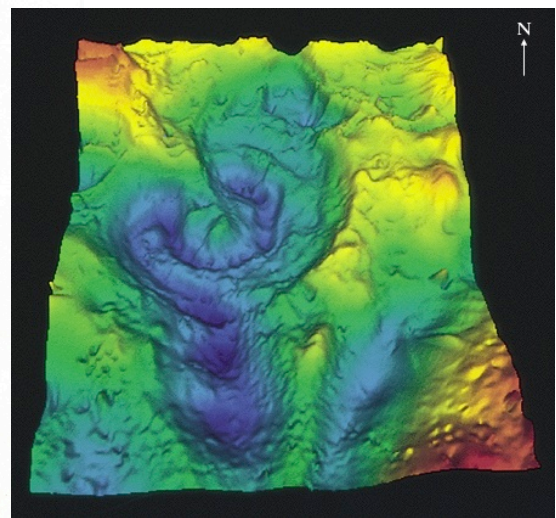
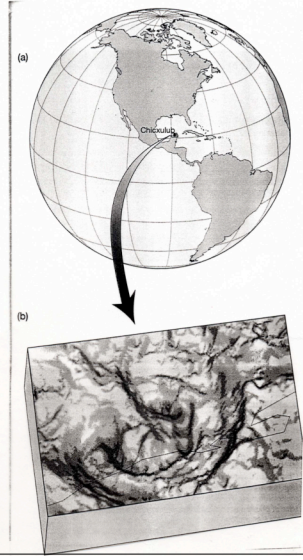
$40 \pm 20 \times 10^4$ metric tons/ yr interplanetary dust accretes every yr!

- 100 m object impacts every 10 kyr
- 10 km object every 100 Myr

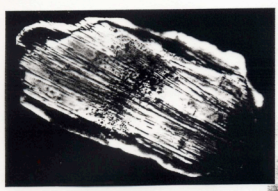
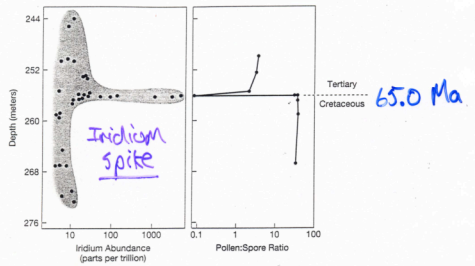
Kump et al. (1999)

Chicxulub Crater Gulf of Mexico

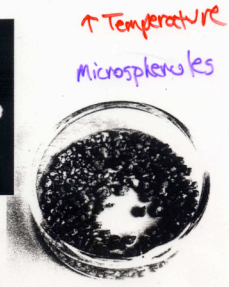
- 200 km crater
- 10-km impactor
- 65 Myr BP
- Extinction of 75% of all species!



Evidence for Meteorite Impact @ K-T Boundary



↑ Pressure
Shocked Quartz



↑ Temperature
Microspores

Phanerozoic History of Extinctions

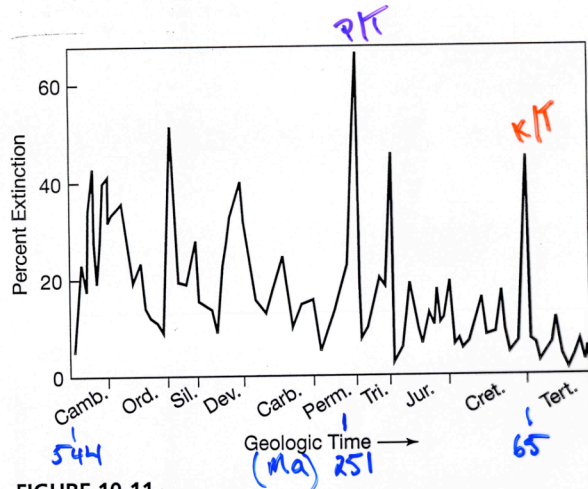
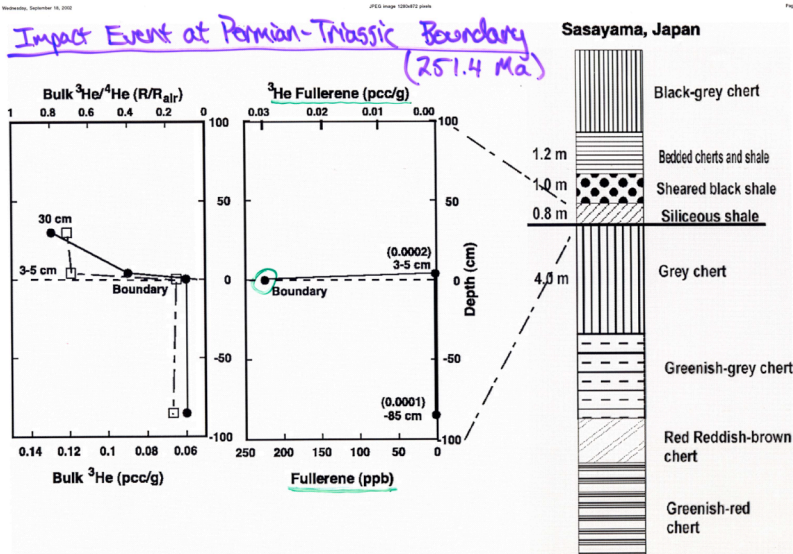
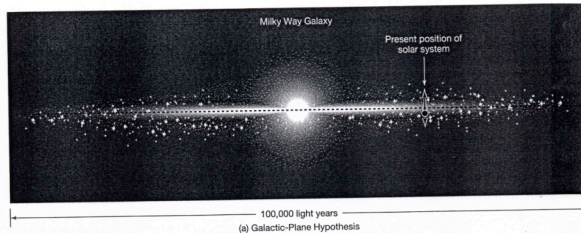


FIGURE 10-11

The fossil record of extinction rate, shown as the percentage of existing genera that went extinct in a particular interval (*stage*) of geologic time. (After Sepkoski, J.J. Jr., *Geotimes*, March, 1994, 15-17.)



Becker et al. (2001), *Science*, 291: 1530-1533



26 Myr Period of Extinctions? Astronomical Hypotheses

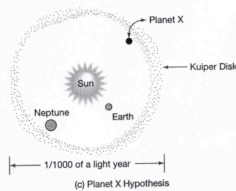
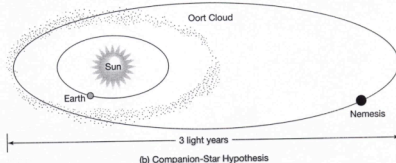


FIGURE 10-12
Three astronomical hypotheses explaining the 26-million-year periodicity in the fossil record of extinction. Figures not drawn to scale. (After Raup, D.M., 1986. See Further Reading.)

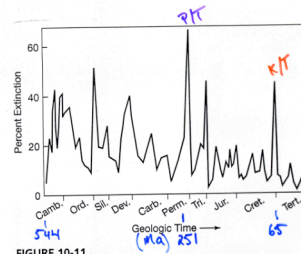
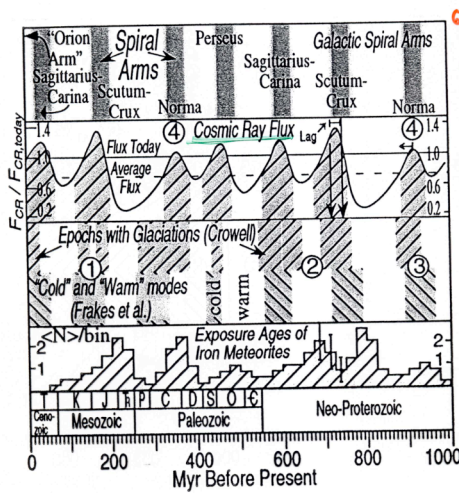


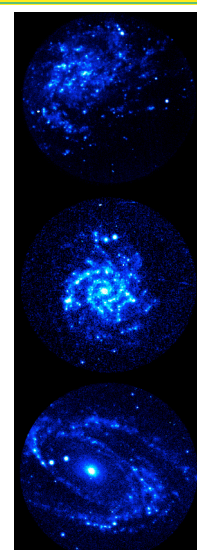
FIGURE 10-11
The fossil record of extinction rate, shown as the percentage of existing genera that went extinct in a particular interval (stage) of geologic time. (After Sepkoski, J.J. Jr., *Geotimes*, March, 1994, 15-17.)

Kump et al. (1999)



Galactic spiral arm crossings
Cosmic Ray Flux
Glacial Epochs

Cosmic Ray Forcing of Climate?



Shaviv (2002), *Phys. Rev. Lett.*, v. 89(5): 051102-1-4

$\frac{FCR}{FCR_{today}} : 25\% - 135\%$
+10 -5 K

<http://antwrp.gsfc.nasa.gov/apod/ap960409.html>

Cosmic Ray Influence on Climate?

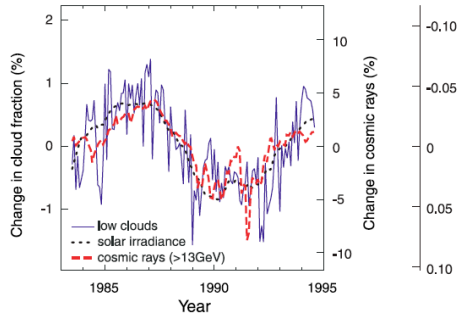


Fig. 1. Variation of low-altitude cloud cover, cosmic rays, and total solar irradiance between 1984 and 1994. The cosmic ray intensity is from Huancaayo observatory, Hawaii. [Adapted from (4)]

Carlsaw et al. (2002) *Science* Vol. 298: 1732-1737.

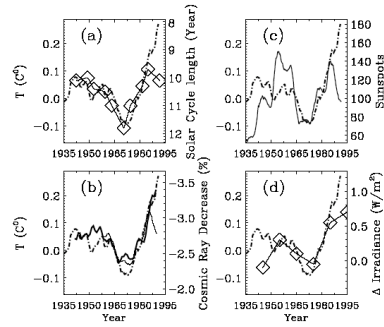
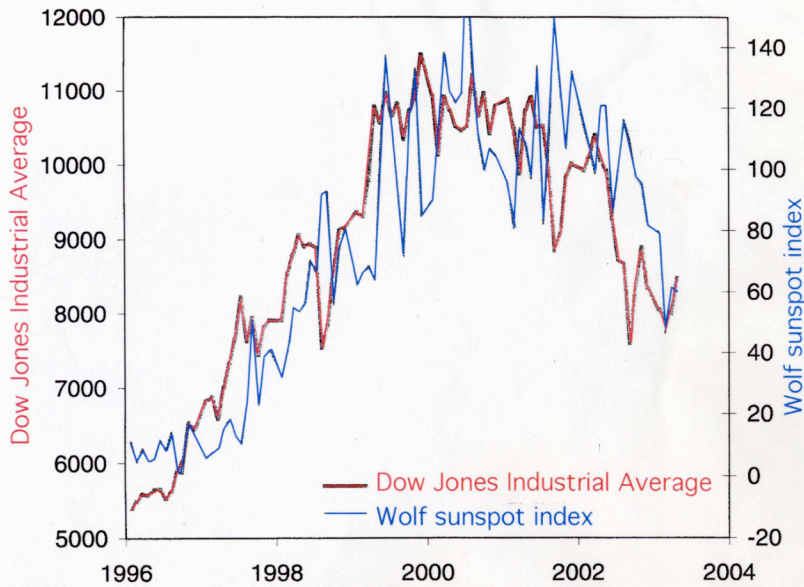


FIG. 3. 11 year average of northern hemispheric marine and land temperatures (dash-dotted line) compared with (a) unfiltered solar cycle length; (b) 11 year average of cosmic ray flux (from ion chambers 1937–1994, normalized to 1965), thick solid line; the thin solid line is cosmic ray flux from Climax, Colorado neutron monitor (arbitrarily scale); (c) 11 year average of relative sunspot number; (d) decade variation in reconstructed solar irradiance (zero level corresponds to 1367 W/m², adapted from Lean *et al.* [6]). Note the 11 year average has removed the solar cycle in (b) and (c).

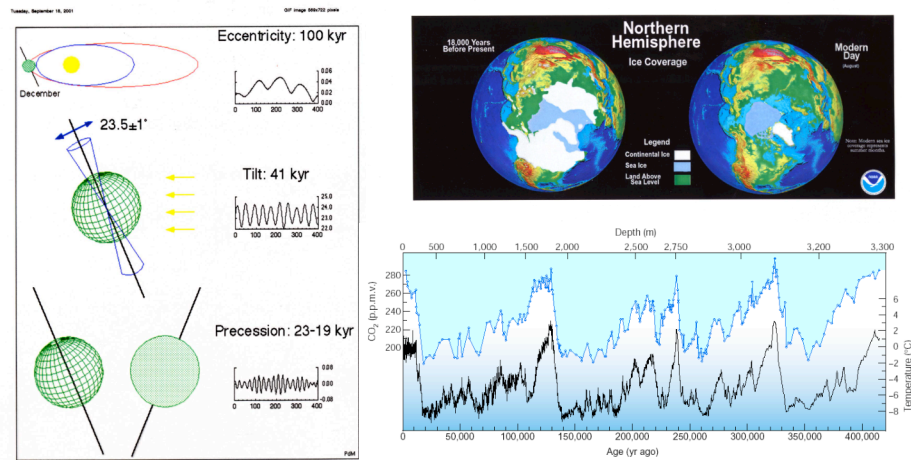
Svensmark (1998) *Phys. Rev. Lett.* Vol. 81(22): 5027-5030.

Correlation Is Not Causation



Earth's Climate Part 4

Pleistocene Glaciations



Earth's Orbital Geometry:

The Milankovitch Hypothesis & the Pacing of Pleistocene Ice Ages

Milankovitch Hypothesis: Historical Perspective

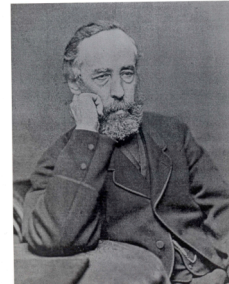
What: Astronomical theory of Pleistocene ice ages.

How: Varying orbital geometry influences climate by changing seasonal & latitudinal distribution of solar radiation incident at top of atmosphere (insolation).

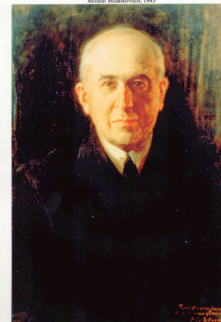
Milestones: Hypothesis

- Croll (1864, 1875): Proposed that variations in seasonal influx of energy--the cumulative affect of eccentricity, obliquity & precession--could trigger large climate response.
- Milankovitch (1920, 1941): Combined laws of radiation with planetary mechanics to derive insolation curves as function of time (600 kyr) and latitude. Concluded summer insolation at high N. lat. (65°N) critical to growth/decay of ice sheets. "The Milankovitch Hypothesis".

James Croll, 1896



Milutin Milankovitch, 1933



Eccentricity, Obliquity (tilt), Precession

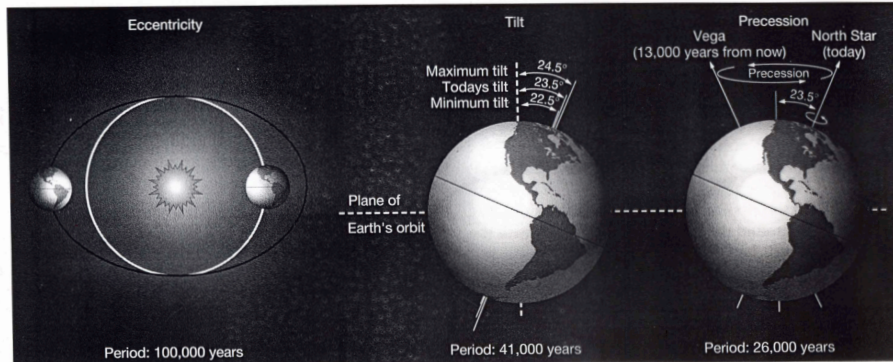
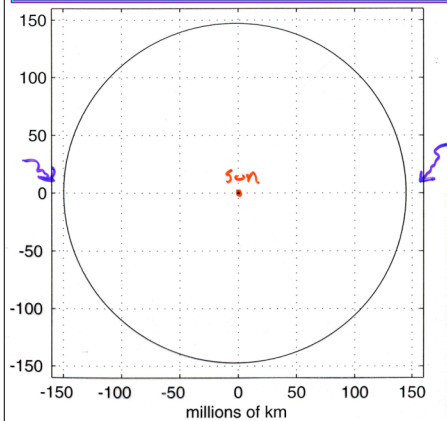


FIGURE 11-5

Aspects of Earth's orbit around the Sun that have implications for climate change. (a) The elliptical nature of the orbit (eccentricity) changes on 100,000-year time scales. (b) The tilt of the spin axis with respect to the plane of Earth's orbit around the Sun (obliquity) changes on a 41,000-year time scale. (c) The orientation of the spin axis in space wobbles (precesses) with periodicities of 19,000 and 23,000 years. (From J.P. Davidson, W.E. Reed, and P.M. Davis: *Exploring Earth: An Introduction to Physical Geology*, 1997. Reprinted by permission of Prentice Hall, Upper Saddle River, N.J.)

Kump et al. (1999)

Eccentricity of Present Earth Orbit Around Sun (to Scale)



Present eccentricity = 0.017
Range: 0 - 0.06
100 & 400 kyr periods

Muller & MacDonald (2000)

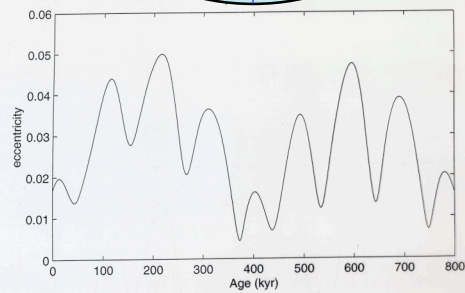


Fig. 2.6. The eccentricity of the Earth's orbit.

Obliquity

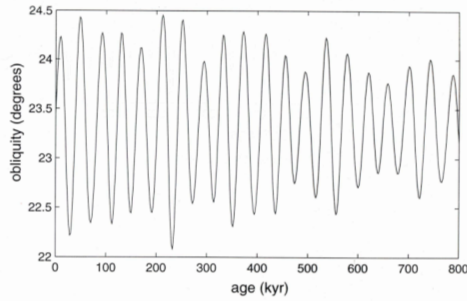
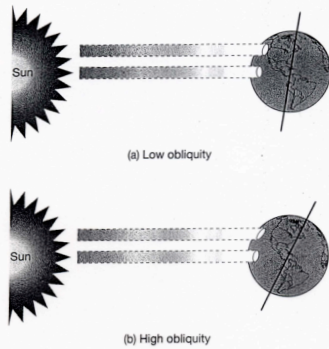


Fig. 2.12. Obliquity.

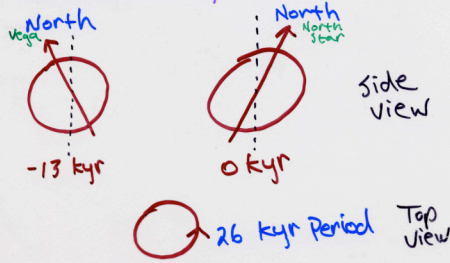
FIGURE 11-7
(a) At low obliquity, Earth has less contrast in insolation between the seasons. (b) At high obliquity, the seasonal contrast is greater.

Muller & MacDonald (2000)

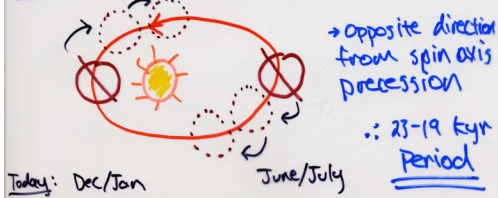
Kump et al. (1999)

2 Types of Precession

I. Precession of Spin Axis



II. Precession of Perihelion



Precession

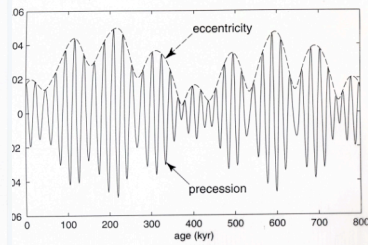
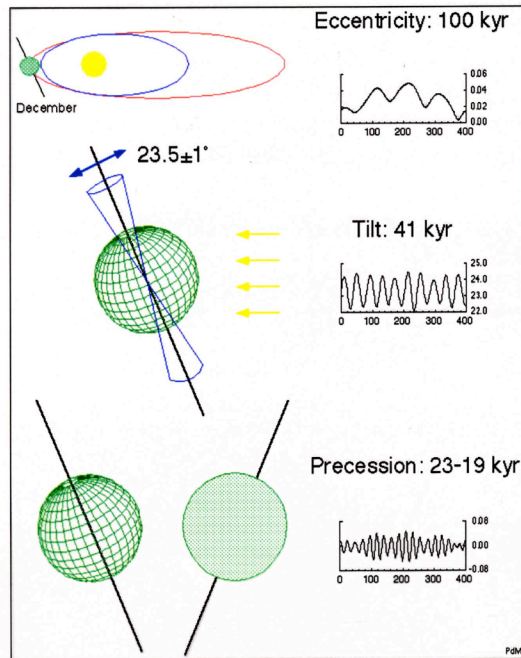
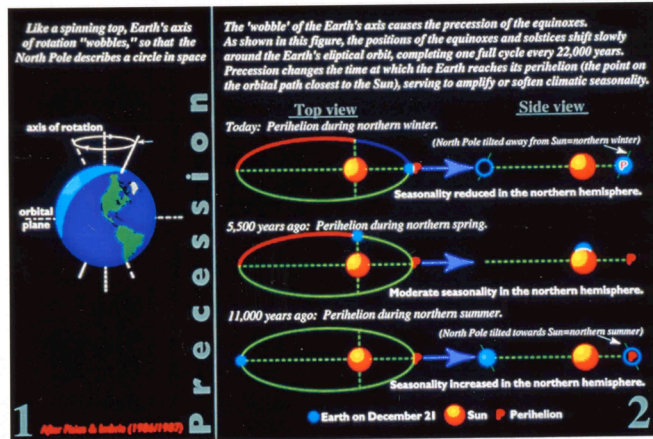


Fig. 2.10. Precession parameter p and eccentricity.

Muller & MacDonald (2000)

Precession of Earth's orbit adapted from Pisias and Imbrie [1986/1987]



Periodic changes in orbital geometry modulate solar radiation receipts (insolation)

Summer (June 21) Insolation at 65°N

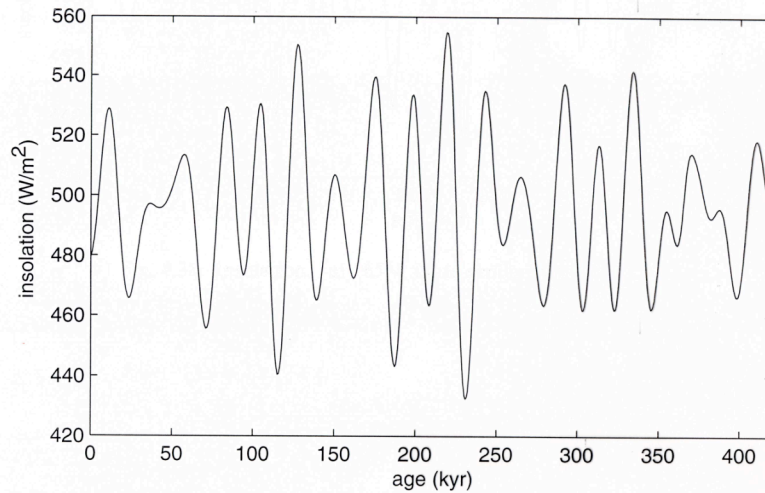
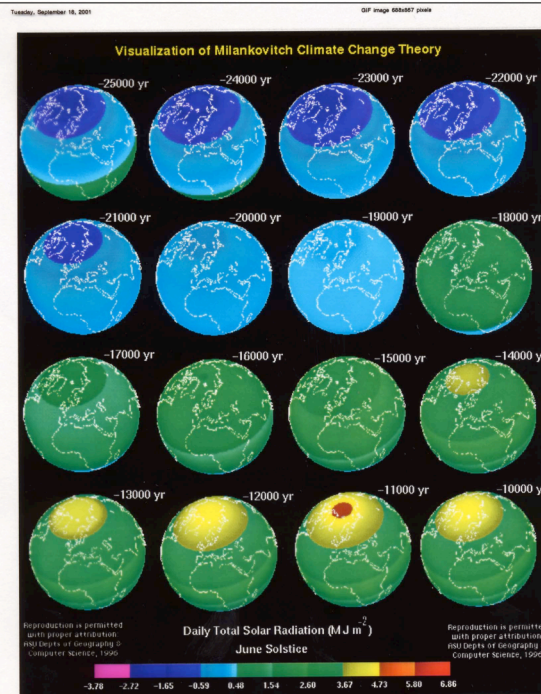


Fig. 4.38. Insolation, July 65N. Note similarity to Fig. 4.37.

Muller & MacDonald (2000)



Increasing
Northern
Hemisphere
insolation
caused the
end of the
last ice age?

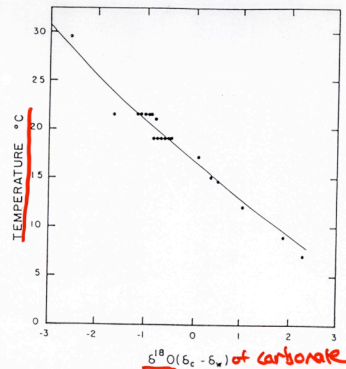
Milankovitch Hypothesis: Milestones & Support

- **Kullenberg (1947):** Invented deep-sea piston coring.
→ Recovery of long, continuous climate records possible.
- **Emiliani (1955):** Pioneered use $^{18}\text{O}/^{16}\text{O}$ ratio of fossil foraminifera in sediment cores as climate (temp.) proxy.
- **Olausson (1965): Shackleton (1967):** Interpret foram $\delta^{18}\text{O}$ changes as whole-ocean isotopic shifts caused by ice sheet growth/decay.
- **1960's:** Recognition of magnetic stripes on ocean floor (geomagnetic field reversals) as global stratigraphic markers.
- **Johnson (1982): Shackleton et al (1990):** Use astronomically-driven insolation variations (E, T, P) to derive timescales for deep-sea cores.
→ Accurately predict age of Brunhes-Matuyama (B/M) magnetic reversal, 780-790 kyr BP. (K/Ar dates for B/M incorrectly placed it at 730 kyr BP.)
- **Baksi et al (1992):** $^{40}\text{Ar}/^{39}\text{Ar}$ date for B/M = 783 kyr BP.
- **Raymo (1997):** Multiple $\delta^{18}\text{O}$ records on 'simple' timescale supports link between N. Hemisphere summer insolation and glacial terminations.

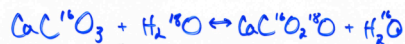
→ Strong support for astronomical influence on climate. (The magnitude of which remains debated...)



T-dependent Isotopic Fractionation



Natural Abundances
 $^{16}\text{O} = 99.756\%$
 $^{17}\text{O} = 0.039$
 $^{18}\text{O} = 0.205$



$$T = 16.9 - 4.2 (\delta^{18}\text{O}_c - \delta^{18}\text{O}_w)$$

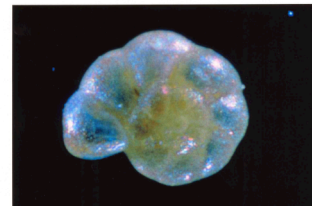
$$\delta^{18}\text{O}_w = f(\text{Salinity, ice volume})$$

$$\delta^{18}\text{O} = \left[\frac{(^{18}\text{O}/^{16}\text{O})_{\text{sample}}}{(^{18}\text{O}/^{16}\text{O})_{\text{standard}}} - 1 \right] \times 1000\text{‰}$$

Epstein et al. (1953)

A Temperature-Dependent Isotopic Fractionation of ^{18}O from ^{16}O Occurs During Calcification

Photo of *Helenina anderseni*



Foraminifera

$\delta^{18}O$ of Seawater varies w/ Salinity

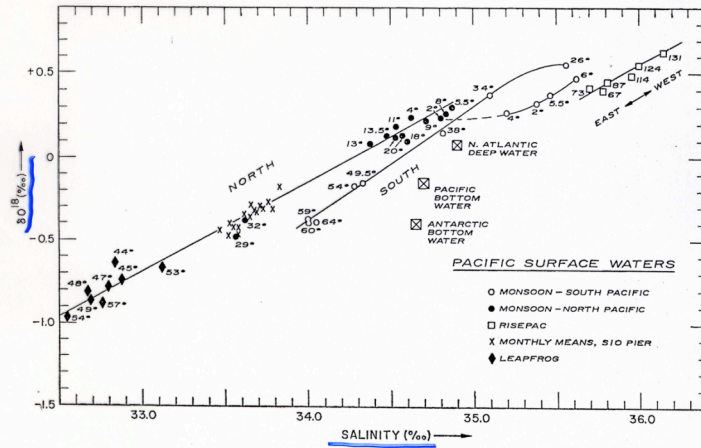
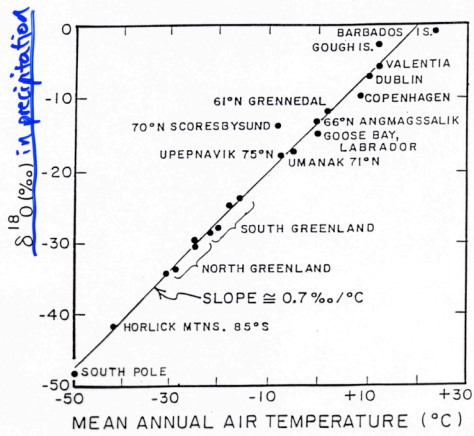


FIGURE 10. — Oxygen 18-salinity relationships in surface and deep Pacific Ocean samples. Latitudes are shown for Monsoon and Leapfrog samples; the figures on the Risepac expedition points are station numbers shown in figure 6.

H. Craig and I. I. Gordon (1965)



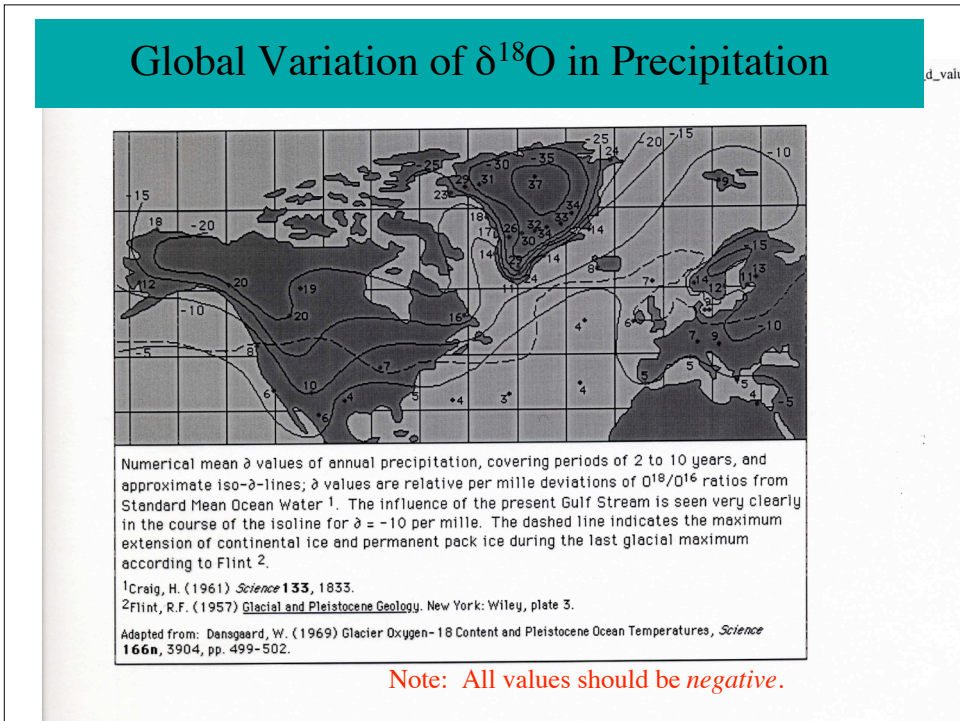
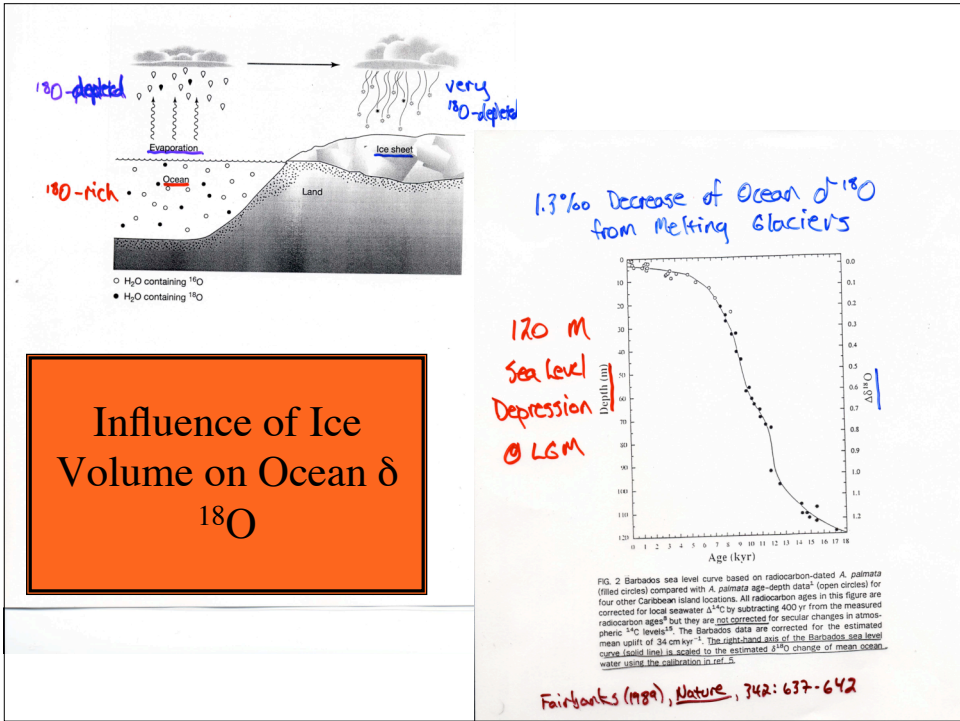
Dansgaard (1964)

• $\delta^{18}O$ of precipitation varies with latitude & altitude.

• Water derived from melting snow & ice is highly depleted in ^{18}O .

• Airmass trajectory influences $\delta^{18}O$ of precipitation

$H_2^{18}O$ has 1% lower vapor P
 \therefore Cold Air (High latitude +/or Altitude) has low $\delta^{18}O$



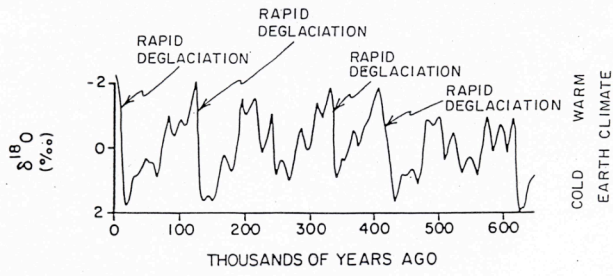
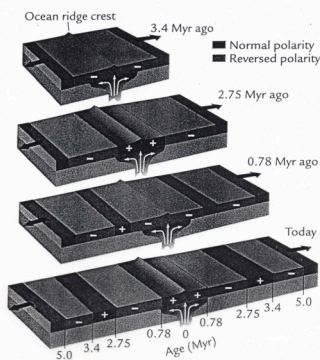


Figure 5. The ^{18}O - ^{16}O record for benthic foraminifera from deep sea sediments. The oxygen isotope results are given as percent difference in the ^{18}O to ^{16}O ratio from that in an international reference standard. The more positive the $\delta^{18}\text{O}$ value the larger the ^{18}O content of sea water. As the growth of ice caps enriches sea water in ^{18}O , these high values correspond to times of large continental ice cover. The time scale was obtained from radioisotope measurements on the deep sea sediments. Although not a regular progression, the times of large ice cover follow one another at roughly 100,000 year intervals. Note also the rapidity with which the largest of these ice masses disappeared!

Magnetic Stripes



Magnetic Stratigraphy



FIGURE 5-8 Magnetization of ocean crust Successive bands of ocean crust form as molten lava erupts at the seafloor, cools, and solidifies. The new crust is magnetized in the normal or reversed polarity prevailing at the time. As the plates move apart, equal amounts of magnetized crust are carried away from the ridge axis in both directions and can be used to date the seafloor. (Modified from F. Press and R. Siever, *Understanding Earth*, 2nd ed., © 1998 by W. H. Freeman and Company.)

- ① $^{40}\text{Ar}/^{39}\text{Ar}$ - date Lava Flows
- ② Apply dates to downcore reversals

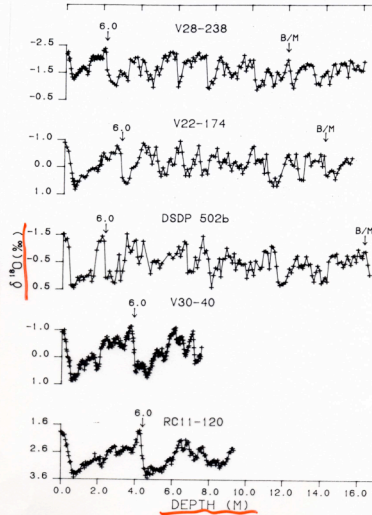


Figure 4 Variations in $\delta^{18}O$ as a function of depth in five deep-sea cores. Two important stratigraphic levels are labeled as follows: 6.0 for the boundary between isotope stages 5 and 6; and B/M for the magnetic reversal at the Brunhes-Matuyama boundary. See Table 1.

Imbrie et al. (1984)

Simple Timescale

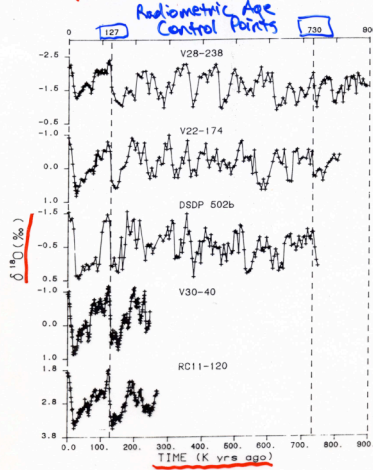


Figure 5 Variations in $\delta^{18}O$ as a function of estimated time in five deep-sea cores. The time scale is derived by linear interpolation between (and extrapolation beyond) control points at 127 KY, 730 KY BP. For details, see text and Table 5.

Imbrie et al. (1984)

Filter of $\delta^{18}O$ Record at Obliquity
+ Precession Frequencies

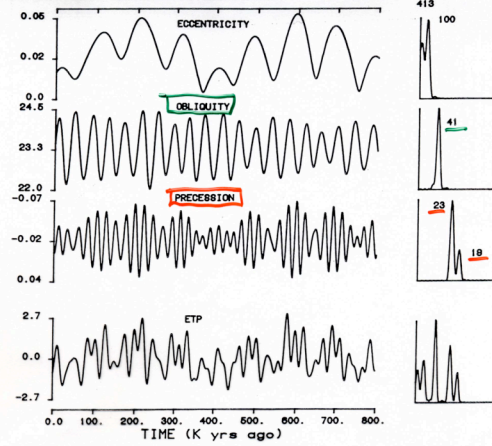


Figure 2 Variations in eccentricity, obliquity, and the precession index ($\Delta e \sin \omega$) over the past 800 000 years. Left: The three upper time series are from the work of Berger (1). These have been normalized and added to form the curve labeled ETP. The scale for obliquity is in degrees; for ETP, in standard deviation units. Right: Variance spectra calculated from these time series, with the dominant periods (KY) of conspicuous peaks indicated.

Imbrie et al. (1984)

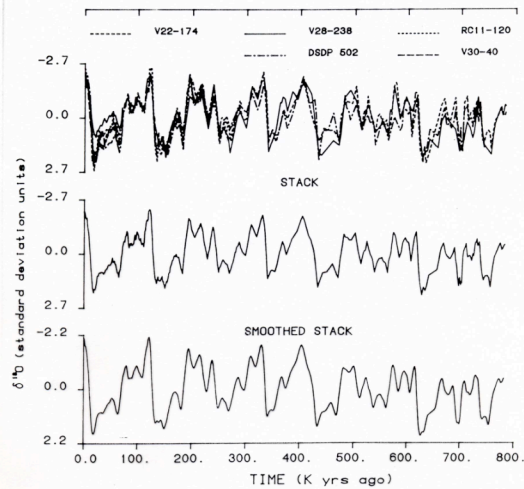
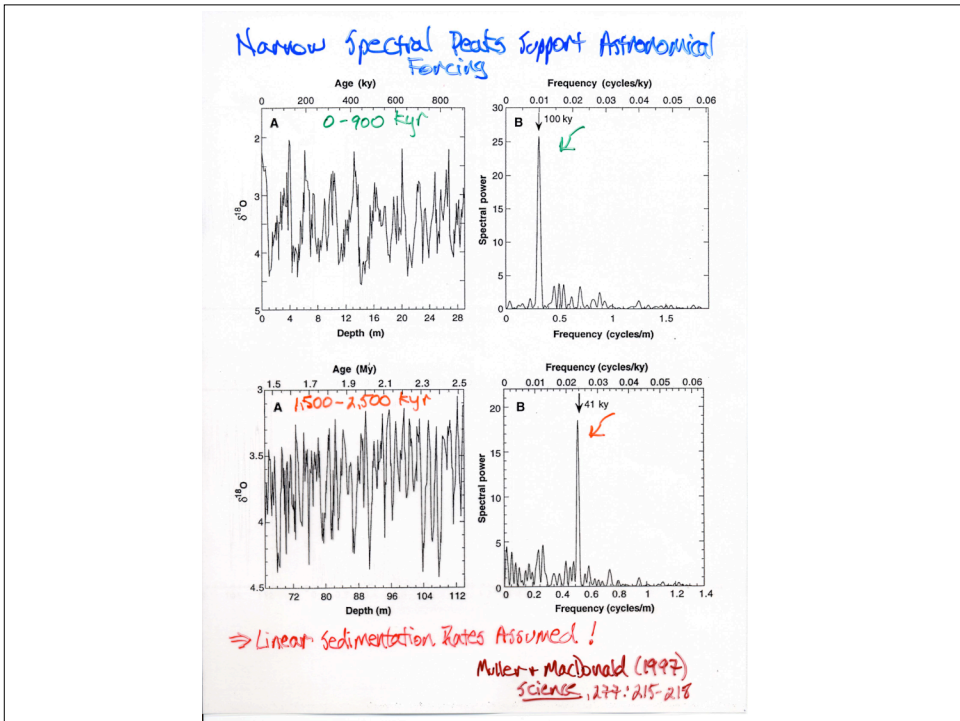
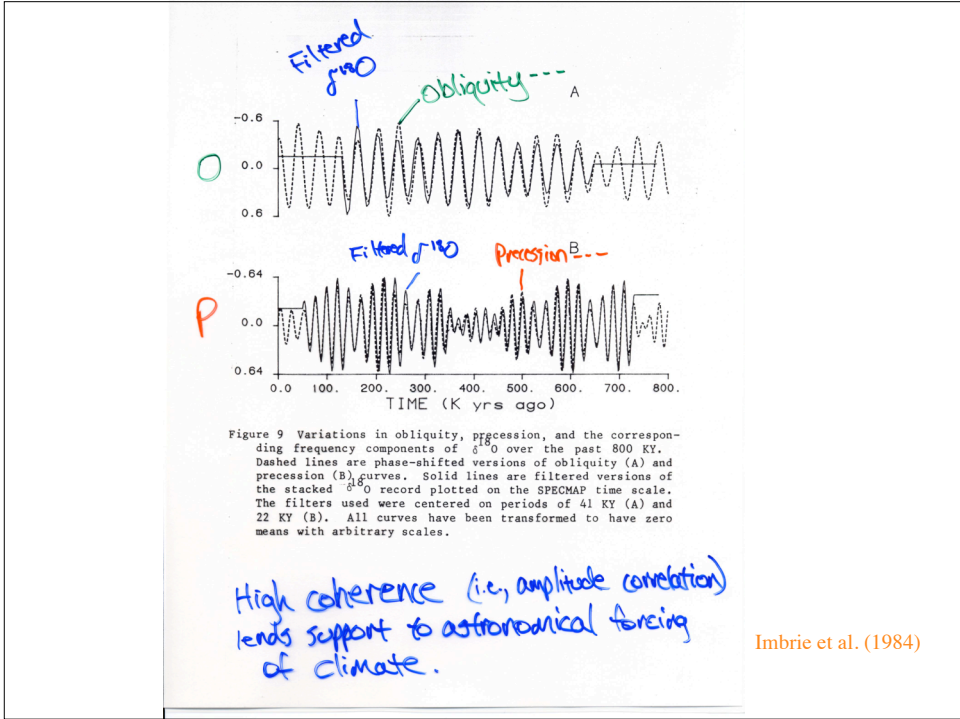


Figure 8 $\delta^{18}O$ variations in five deep-sea cores normalized and plotted on the SPECMAP time scale. In the top panel, data from each core has been normalized to zero mean and unit standard deviation. After interpolation at intervals of 1 KY, these curves have been averaged (middle panel), and smoothed with a 9-point Gaussian filter (bottom panel).

Imbrie et al. (1984)



1. Why is climate response in 100-kyr band so strong?

Observation: High correlation of $\delta^{18}\text{O}$ cycles with astronomically-driven radiation cycles at E, T & P frequencies suggests causal link in all 3 bands.

Problem: Amplitude of insolation change (~0.2%) is ~10x smaller than in T,P bands.

Possible Solution: E modulates climatic effect of P. High E favors NH glaciation when P causes NH summer to occur at maximum Earth-Sun distance (i.e., Imbrie et al, 1993).

2. Why do glacial cycles switch from 41-kyr to 100-kyr period ~700 kyr BP?

Possible solution: L/T cooling trend, perhaps from tectonically-driven decrease in atmospheric CO_2 , facilitates NH ice sheet growth beyond a critical threshold during insolation minima. These large ice sheets drive climate through feedbacks internal to the climate system (geo-, cryo-, atmo-, hydro-sphere).

3. Why do full glacial Terminations, and ensuing interglacial periods, occur ~430 and ~15 kyr BP when E is very low?

-**Possible solution:** 100-kyr cycle of orbital inclination (Muller and MacDonald, 1995).

-**Caveat:** no obvious mechanism linking climate to inclination.

Milankovitch Hypothesis Challenges:

100-kyr Cycle Problems

Eccentricity Modulates Precession

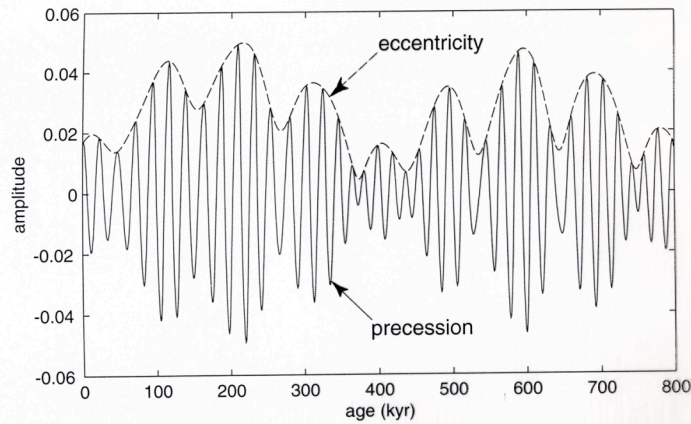


Fig. 2.10. Precession parameter p and eccentricity.

$$p = e \sin \omega$$

ω = \angle between Spring Equinox + perihelion

Muller & MacDonald (2000)

100-Kyr Cycle Problem-1

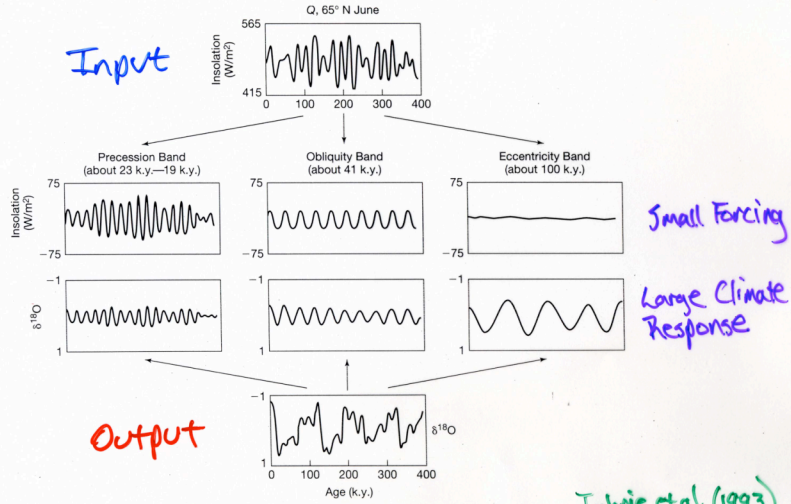
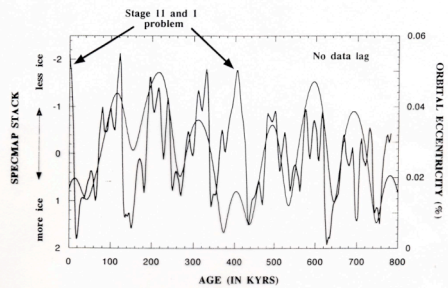
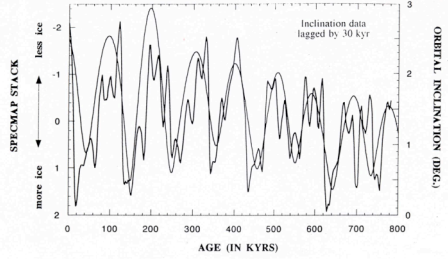


FIGURE 11-9 Northern Hemisphere June insolation (Q , the climate forcing) and marine oxygen isotopic composition ($\delta^{18}O$, the climate response) and their dominant periodic components. (After Imbrie et al., *Paleoceanography* 7:701-738, 1992.)

100 kyr Climate Forcing from Orbital Inclination?



Muller & MacDonald (1995), *Nature*, v. 377: 107-108

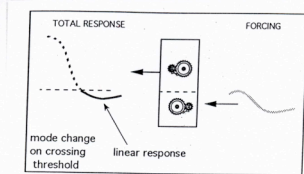
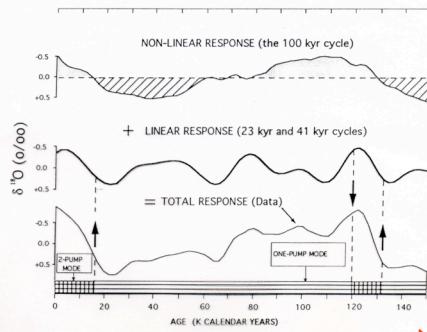


Fig. 17. Model of a nonlinear amplification mechanism. The system's gain is sharply increased when the linear response to an external forcing crosses a threshold.



Imbrie et al. (1993)

The 100 kyr Cycle Problem - 2

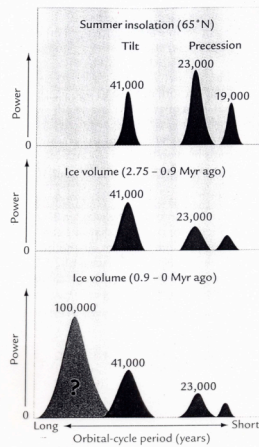
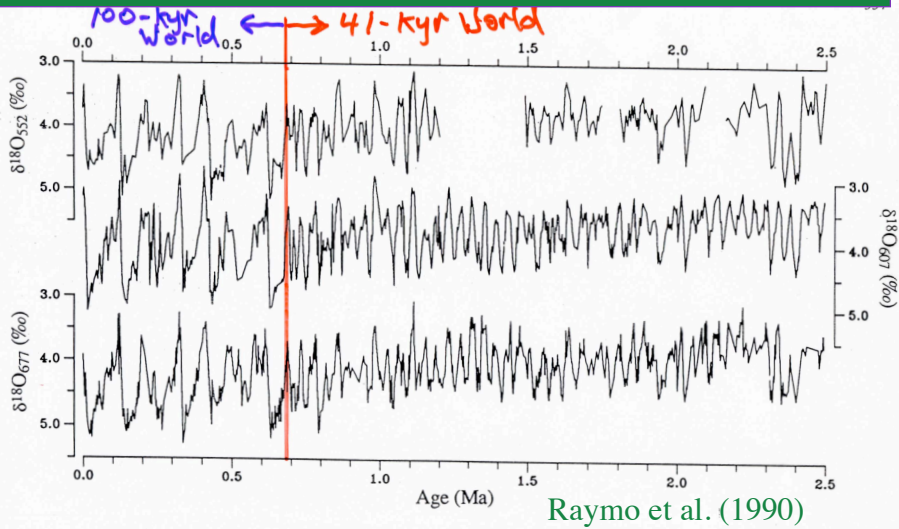


FIGURE 10-17 Spectral analysis: insolation and ice volume. Summer insolation changes at 65°N occur only at the orbital rhythms of tilt (41,000 years) and precession (23,000 and 19,000 years) (top). Between 2.75 and 0.9 Myr ago, the $\delta^{18}\text{O}$ signal (northern hemisphere ice volume and deep-ocean temperature) contains the same rhythms as orbital insolation (middle). The large 100,000-year cycle evident in the $\delta^{18}\text{O}$ (ice volume) signal since 0.9 Myr ago is not present in the insolation signal (bottom).

Pleistocene Ice Age Cycles



"100-kyr Ice"

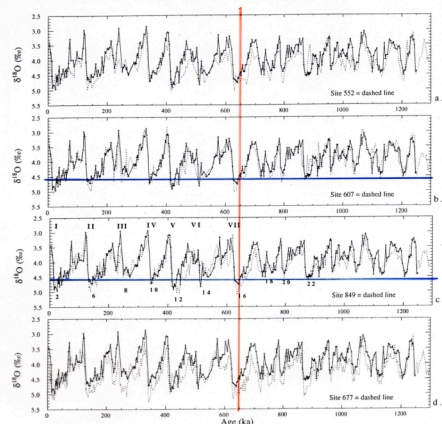


Figure 4. Oxygen isotope data (replicates averaged and species adjustments made) from sites 552, 607, 664, 849, and 677. The site 664 record is plotted on each panel to facilitate evaluation of correlations between these five sites. The horizontal lines in Figures 4b and 4c define the limits of "100K ice," the added ice volume which characterizes the Broecker "100 ka world." In Figure 4c the major terminations of the late Pleistocene are labeled (I-VII), as are selected marine oxygen isotope stages.

Raymo et al. (1997)

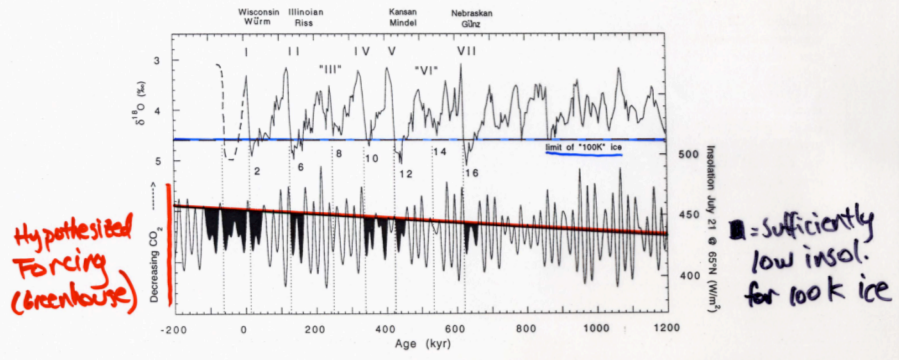
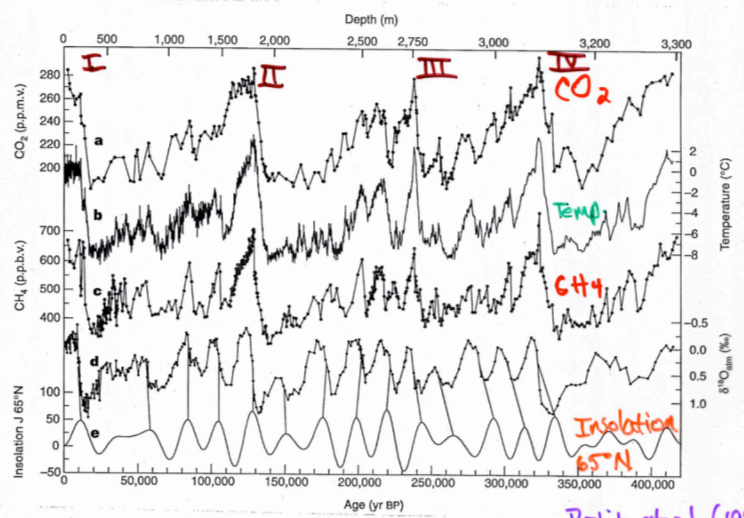


Figure 5. Benthic $\delta^{18}\text{O}$ data from Pacific Site 849 plotted to the GSS97 timescale. Insolation received on July 21 at 65°N is shown on lower half of figure [after Laskar *et al.*, 1993]. This site is representative of the pattern of ice volume change over the last 800 kyr and can be compared with other records plotted in Figure 1. The horizontal dashed line on the $\delta^{18}\text{O}$ record indicates the level below which 100-kyr ice is observed. Terminations and selected isotope stages are labeled, as well as the historical names of the glacial stages. On the insolation record, the fiducial level below which 100-kyr ice can nucleate and be stable (shaded regions) is indicated by the slanted horizontal line. The vertical dashed lines indicate the midpoint of terminations using the GSS97 timescale.

Raymo (1997)

420,000 Years of Climate at Vostok, Antarctica



Petit *et al.* (1999)